CZECH TECHNICAL UNIVERSITY IN PRAGUE

Faculty of Nuclear Sciences and Physical Engineering

Department of Physics

Research Project

Study of the properties of charm mesons with HFT detector

Bc. Jakub Kvapil

Supervisor: Mgr. Jaroslav Bielčík, Ph.D.

Consultant: Ing. Miroslav Šimko

Prague, 2016

ČESKÉ VYSOKÉ UČENÍ TECHNICKÉ
V PRAZE
Fakulta jaderná a fyzikálně inženýrská
Katedra fyziky

Výzkumný úkol

Studium vlastností půvabných mezonů pomocí detektoru HFT

Bc. Jakub Kvapil

Vedoucí práce: Mgr. Jaroslav Bielčík, Ph.D.

Konzultant: Ing. Miroslav Šimko

Praha, 2016

ČESKÉ VYSOKÉ UČENÍ TECHNICKÉ V PRAZE
FAKULTA JADERNÁ A FYZIKÁLNĚ INŽENÝRSKÁ
PRAHA 1 - STARÉ MĚSTO, BŘEHOVÁ 7 - PSČ 115 19

Katedra: fyziky **Akademický rok:** 2015/2016

VÝZKUMNÝ ÚKOL

Posluchač: Bc. Jakub Kvapil

Obor: Experimentální jaderná a částicová fyzika

Vedoucí úkolu: Mgr. Jaroslav Bielčík, Ph.D.

Název úkolu (česky/anglicky):

Studium vlastností půvabných mezonů pomocí detektoru HFT

Study of the properties of charm mesons with HFT detektor

Pokyny pro vypracování:

1. Fyzika těžkých vůní v experimentu STAR
2. Testování HFT simulátoru
3. Rekonstrukce mezonu D+
4. Optimalizace výběrových kritérii pro selekci signálu D+
5. Korekce na geometrickou akceptaci detektoru a účinnost rekonstrukce
6. Spektrum mezonu D+
7. Diskuze a závěr

Výzkumný úkol bude vypracován v anglickém jazyku.
Konzultant: Ing. Miroslav Šimko

Součástí zadání výzkumného úkolu je jeho uložení na webové stránky katedry fyziky.

Literatura:

1. Ramona Vogt, Ultrarelativistic Heavy-Ion Collisions, Elsevier 2007.

2. Riccardo Russo, Measurement of D+ meson production in p–Pb collisions with the ALICE detector, Ph.D. thesis Univeristy of Torino, 2014.
3. A.Andronic et al., Heavy-flavour and quarkonium production in the LHC era: from proton-proton to heavy-ion collisions, arXiv:1506.03981v1.
4. ALICE collaboration, Results on open-charm production in pp, p-Pb and Pb-Pb collisions with ALICE at the LHC, J.Phys.Conf.Ser. 636 (2015) 1, 012003.

Datum zadání: 23.10.2015 ……..

Datum odevzdání: 24.06.2016 ***vedoucí katedry***

Prohlášení:

Prohlašuji, že jsem svou bakalářskou práci vypracoval samostatně a použil jsem pouze podklady (literaturu, projekty, software, atd.) uvedené v přiloženém seznamu.

Nemám závažný důvod proti užití tohoto školního díla ve smyslu § 60 Zákona č. 121/2000 Sb., o právu autorském, o právech souvisejících s právem autorským a o změně některých zákonů (autorský zákon).

V Praze dne 23.6.2016 Jakub Kvapil

Title:
Study of the properties of charm mesons with HFT detector

Author: Bc. Jakub Kvapil

Specialization: Experimental nuclear and partical physics

Supervisor: Mgr. Jaroslav Bielčík, Ph.D.
Consultant: Ing. Miroslav Šimko

Abstract:
The STAR experiment is a part of the Relativistic Heavy Ion Collider located in Brookhaven national laboratory, whose main research task is to study extreme state of nuclear matter and spin of the proton. The Heavy Flavor Tracker vertex detector was installed to STAR experiment in the year 2014 and it drastically improves the STAR's ability to measure open heavy flavor hadrons, e.g. $D^{\pm}$, due to precise reconstruction of secondary vertices and excellent particle identification provided by other detectors.

In order to understand a physics measurement, detector efficiency has to be precisely determined, hence Monte Carlo simulations are made. The aim of this work was to test slow simulator of the STAR Pixel detectors, which are the innermost part of Heavy Flavor Tracker. We report tuning and comparison of the simulator to cosmic and Au+Au 200 GeV/c data.

In this work, $D^{\pm}$ topological reconstruction on Au+Au 200 GeV/c data collected in year 2014 has been made. The decay channel $D^{\pm} \rightarrow K^{\mp}\pi^{\pm}\pi^{\pm}$ was used. Particle identification was done with Time of Flight and Time Projection Chamber and information of secondary vertex was provided from Heavy Flavor Tracker. Combinatorial background was calculated with wrong–sign method. Signal of $D^{\pm}$ was sufficient with total significance of 6.9σ and with new reproduction the significance is 17.7σ.

Key words:
RHIC, STAR, HFT, DIGMAPS, slow simulator, $D^{\pm}$, Run14, Au+Au, 200 GeV

Název práce:
Studium vlastností půvabných mezonů pomocí detektoru HFT

Autor: Bc. Jakub Kvapil

Obor: Experimentální jaderná a částicová fyzika

Vedoucí práce: Mgr. Jaroslav Bielčík, Ph.D.
Konzultant: Ing. Miroslav Šimko

Abstrakt:

STAR experiment je součástí Relativistického srážeče těžkých iontů v Brookhavenské národní laboratoři, jehož hlavním cílem je zkoumat extrémní stavy hmoty a spin protonu. Vertexový detektor Heavy Flavor Tracker byl na experiment STAR nainstalován v roce 2014 a umožňuje měření částic s otevřenou těžkou vůní, např. $D^{\pm}$, díky velmi přesnému rozlišení sekundárních vertexů a identifikaci částic.

Pro dobré porozumění fyziky je potřeba přesně určit efektivitu detektorů, která se určuje pomocí Monte Carlo simulací. Cílem je otestovat tzv. pomalý simulátor pixelových detektorů, které tvoří nejcentrálnější vrstvy detektoru Heavy Flavor Tracker. Testování bylo provedeno na kosmických datech a Au+Au 200 GeV/c srážkách.

V této práci byla provedena topologická rekonstrukce $D^{\pm}$ na Au+Au 200 GeV/c datech nasbíraných v roce 2014. Byl použit rozpadový kanál $D^{\pm} \rightarrow K^{\mp}\pi^{\pm}\pi^{\pm}$. Identifikace částic byla provedena za pomoci Detektoru doby letu a časově projekční komory a na přesné určení sekundárních vertexů byl použit detektor Heavy Glavor Tracker. Kombinatorické pozadí bylo vypočítáno metodou špatné nábojové kombinace. Signál $D^{\pm}$ má signifikanci 6.9σ a s novou reprodukcí dokonce 17.7σ.

Klíčová slova:
RHIC, STAR, HFT, DIGMAPS, slow simulator, $D^{\pm}$, Run14, Au+Au, 200 GeV

Acknowledgement

I would like to thank Mgr. Jaroslav Bielčík, Ph.D. for his help, patience, and support and Ing. Miroslav Šimko for being helpful 24/7, for correcting my research project and providing grammatical control. I also want to thank my colleagues, family and friends, who supported me.

Contents

List of Figures

List of Tables

Chapter 1

Introduction

This work is dedicated to the ongoing research in Brookhaven National Laboratory at Relativistic Heavy Ion Collider (RHIC) and STAR detector. One method of studying the extreme state of nuclear matter are colliding experiment. The particles are accelerated to high velocity and collided with target or other accelerated particle. The collision energy is released to the production of new particles which are measured by detectors.

Second chapter describes RHIC accelerator and its future plans, STAR detector with most important mid rapidity subdetectors and importance of the most central detector layers (Heavy Flavor Tracker–HFT) to tracking resolution with D^0 as example. Heavy Flavor Tracker two most innermost layer are pixel detectors build by MAPS technology, this is the first time MAPS technology was used in a collider experiment.

In order to understand physical measurements, detector efficiency need to be precisely determined. A new slow simulator has been developed, a simulator capable of simulation on the level of single pixels. This is the content of the third chapter. First, simulation physics and principle is shown. Next, a code structure of standalone DIGMAPS, running commands and input parameters are described. Moreover, calibration on cosmic muon measurement is mentioned. Finally, low luminosity data testing and code improvement is shown.

Forth chapter is dedicated to second research task – $D^{\pm}$ meson reconstruction. $D^{\pm}$ reconstruction with Heavy Flavor Tracker on year 2014 Au+Au 200 GeV data has been made. Before HFT was installed at STAR in year 2014 the D mesons was reconstructed only with help of Time of Flight (TOF) and Time Projection Chamber (TPC). It was not possible to measure $D^{\pm}$, however with help of HFT with topological reconstruction one can measure three–body decays. As a complement measurement to the D^0, the $D^{\pm}$ information provides additional probe to the behaviour of the c quark in the medium.

Chapter 2

Solenoidal Tracker at RHIC

In this chapter, the Relativistic Heavy Ion Collider (RHIC) is described including up to date experimental plans for the next two years (2017 and 2018). STAR experiment and its main mid rapidity detectors is shown, i.e. Muon Telescope detector, Barrel Electromagnetic Calorimeter, Time of Flight, Time projection Chamber and Heavy Flavor Tracker – Silicon Strip Tracker, Intermediate Silicon Tracker and Pixel detectors. Finally, the importance of the Heavy Flavor Tracker at STAR is shown with respect to heavy flavor measurements.

2.1 Relativistic Heavy Ion Collider (RHIC)

The Relativistic Heavy Ion Collider (RHIC) is located in the Brookhaven National Laboratory (BNL) in Upton, New York and started its operation in the year 2000. After the Large Hadron Collider (LHC), it is the second largest particle accelerator in the world. Furthermore, it is the only accelerator capable of colliding polarised protons. The current spokesperson of the STAR experiment is Zhangbu Xu [1].

RHIC is a so called storage ring collider, two independent rings are filled with particles, accelerate them in opposite direction and collide them in interaction point. The collider can hold and collide particles up to 10 hours and can accelerate different types of positively charged ions. The accelerator has a hexagonal shape, is 3834 m long, contains 1740 Ni-Ti superconducting magnets with the magnetic field of 3.45 T to bend the beam trajectory. RHIC contains a total of 6 interaction points where rings intercept. Each interaction point are numbered as a clock. At 6 o'clock, the injector and the STAR (Solenoidal Tracker at RHIC) experiment are located and at 8 o'clock is the location of the PHENIX experiment and will be shut down with end of this year run. Experiment PHOBOS located at 10 o'clock shut down its operation in the year 2005 and experiment BRAHMS located at 2 o'clock in the year 2006 [1].

Before injection into RHIC, particles must be pre-accelerated, this is done in several steps:

1. For ions a so called Electron Beam Ion Source (EBIS) (2 MeV/nucleon in the case of Au) and for protons a 200 MeV Linear accelerator (Linac) is used,

2. Booster synchrotron – 100 MeV/nucleon in the case of Au,

3. Alternating Gradient Synchrotron (AGS) – 8,86 GeV/nucleon in the case of Au.

RHIC is able to accelerate and collide many types of ions e.g. p+p, d+Au, He3+Au, Cu+Cu, Cu+Au, Au+Au, U+U [2]. Gold can be collided at central mass energy $9.2 - 200$ GeV per nucleon pair at $85 \cdot 10^{28}$ cm^{-2}s^{-1} luminosity (year 2015). RHIC's special feature is that it can collide polarized protons. In year 2013, RHIC reached up to 52 % p+p polarization at 500 GeV and $160 \cdot 10^{30}$ cm^{-2}s^{-1} luminosity. Ability to collide polarized systems is essential for the current and future research of the proton spin. Basic informations about the RHIC accelerator are in Table 2.1 and a photograph of the complex with marked individual pre-accelerators is shown in Figure 2.1.

2.2 RHICs future

For year 2017 (Run17) STAR collaboration proposed 13 weeks of transverse polarised p+p at 500 GeV and one week p+p at 500 GeV. Also 2 weeks is designated to Coherent electron Cooling (CeC), as a novel form of electron cooling. This test is part of preparation for future eRHIC era. Remaining 4 weeks are designated to Au+Au at 62.4 GeV [6].

Year 2018 (Run18) is designated to isobaric nucleus measurements, 3.5 weeks of Ru+Ru at 200 GeV and 3.5 weeks of Zr+Zr at 200 GeV in order to understand the phenomenon of chiral magnetic effects [7]. Run will be ended by 2 weeks of Au+Au at 27 GeV [6] as a part of critical point study.

It is worth mentioning that a new collaboration RHICf [8](RHIC forward) was created. It will use a calorimeter build for future The Compressed Baryonic Matter (CBM) experiment at Facility for Antiproton and Ion Research (FAIR). Calorimeter was installed at forward STAR region and will use STARs DAQ. The main physics programme is to study single spin asymmetry and cross section of forward particle to understand cosmic ray air showers. Measurement will be taken during year 2017 .

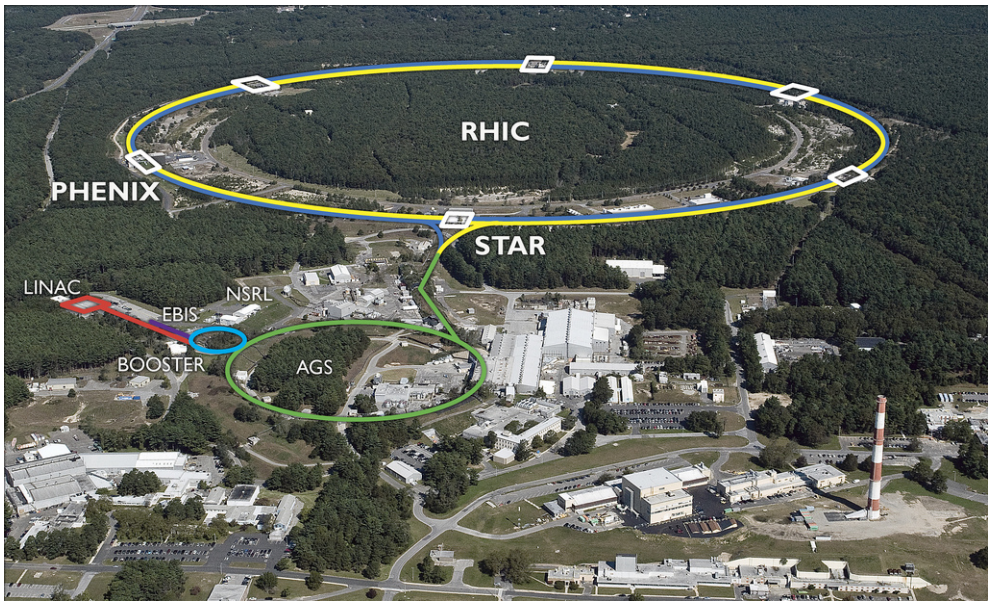

Figure 2.1: Photograph of the RHIC facility with marked individual pre-accelerators. One RHIC ring is labeled yellow other one blue. Taken from Ref. [3].

Circumference	3833.845 m
No. of interaction points	6
No. of dipole magnets	396
No. of quadrupole magnets	492
Dip. mag. magn. field @ 100GeV/n Au	3.458 T
Dip. mag. current	5.093 kA
Operation temperature (Helium coolant)	< 4.6 K
Cooling power at 4 K	24.8 kW
Time needed to cooling the system from 50 K	0.5 week
Au operating lifetime	10 h
No. of bunch/ring	111
No. of ions/bunch	$1.6 \cdot 10^9$
Beam energy	560 kJ
Kinetic energy (each beam): p	$31.2 - 250$ GeV
Kinetic energy (each beam): Au	$4.6 - 100$ GeV/N
Average luminosity, Au @ 100 GeV/N	$50 \cdot 10^{26}$ cm^{-2}s^{-1}

Table 2.1: Basic informations about the RHIC accelerator. Taken from Ref. [2,4,5].

2.3 STAR Detector

The main barrel of the STAR detector (Solenoidal Tracker At RHIC) consists of several central mid-rapidity sub-detectors [9]. Gradually from periphery to the centre:

- Muon Telescope Detector – MTD,
- Barrel Electromagnetic Calorimeter – BEMC,
- Time of Flight – TOF,
- Time Projection Chamber – TPC,
- Silicon Strip Tracker – SSD,
- Intermediate Silicon Tracker – IST,
- Pixel detector – PXL.

The last 3 named are part of a unit called (Heavy Flavor Tracker – HFT). STAR detector is shown in the Figure 2.2.

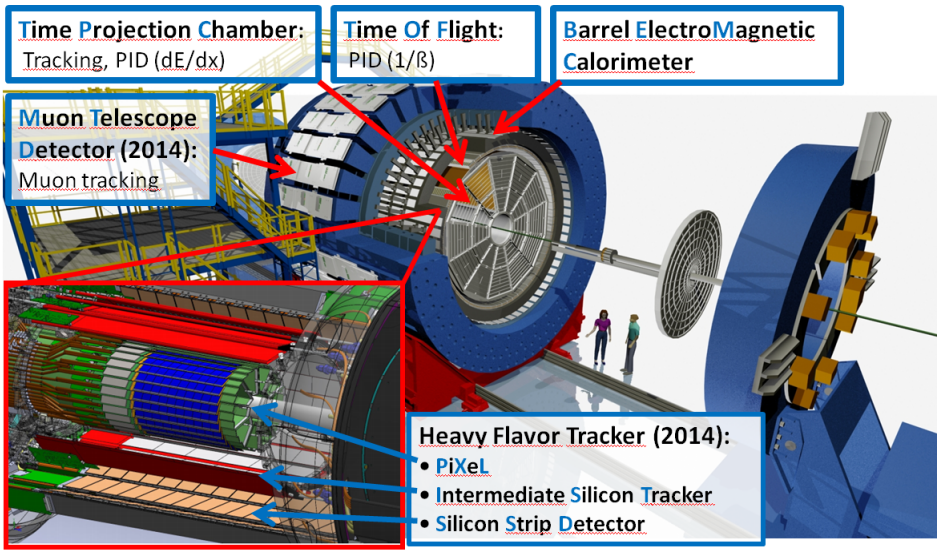

Figure 2.2: STAR detector with sub-detectors.

2.3.1 Muon Telescope Detector

Muon Telescope Detector (MTD) is located on the outer side of the STAR magnet, 400 cm far from interaction point. Muons easily traverse through STAR magnet unlike other particles thus we can exploit this property to identify muons from other particles, and measure Υ and J/ψ mesons trough di–muon decays. Basic specification are in Table 2.2.

Azimuthal coverage	45 %
Pseudorapidity coverage	$\lvert\eta\rvert \leq 0.5$
Time resolution	$\leq$100 ps
Spartial resolution	$\sim$ 1 cm
Number of channels	2808

Table 2.2: Specification of STAR MTD. Taken from Ref. [10, 11].

2.3.2 Barrel Electromagnetic Calorimeter

Barrel Electromagnetic Calorimeter (BEMC) is located on the inner side of the magnet at 220 cm. The calorimeter includes Barrel Shower Maximum detector (BSMD) is used for measuring γ from π^0 decay. Its other purposes are e.g. direct γ and electrons identification and jets. It is divided into towers and each tower consists of scintillation and lead layers. Basic specification are in Table 2.3.

Inner radius	$\approx$ 220 cm
Length	586 cm
Pseudorapidity coverage	$\lvert\eta\rvert \leq 1$
Number of towers	4800
Scintillation layers per tower	19 $\times$ 5 mm 2 $\times$ 6 mm
Lead layers per tower	20 $\times$ 5 mm

Table 2.3: Specification of STAR BEMC. Taken from Ref. [12].

2.3.3 Time of Flight

Time of Flight (TOF) detector is located between the calorimeter and Time projection Chamber covering full azimuthal angle and pseudorapidity $\eta \leq 1$ [13]. It consists of 120 Multigap Resistive Plate Chambers (MRPC)–glass plates with gas for proportional amplification. TOF is used for the measurement of time of flight of particles Δt, while the initial time is taken from pVPD. The Time Projection Chamber (TPC) provides the particle momentum and flight path Δs, together with these three pieces of information one can identify the particles using following equations

$$\frac{1}{\beta} = c\frac{\Delta t}{\Delta s} \tag{2.1}$$

and

$$m = \frac{p}{c}\sqrt{\left(\frac{1}{\beta}\right)^2 - 1}. \tag{2.2}$$

TOF can precisely identify particles with low momenta, thus complements the TPC. Inverse velocity $1/\beta$ as function of transverse momentum p_T is shown in Figure 2.3. Intercept histogram is shown for momenta in the range of $1.2 < p_T < 1.4$ GeV/c.

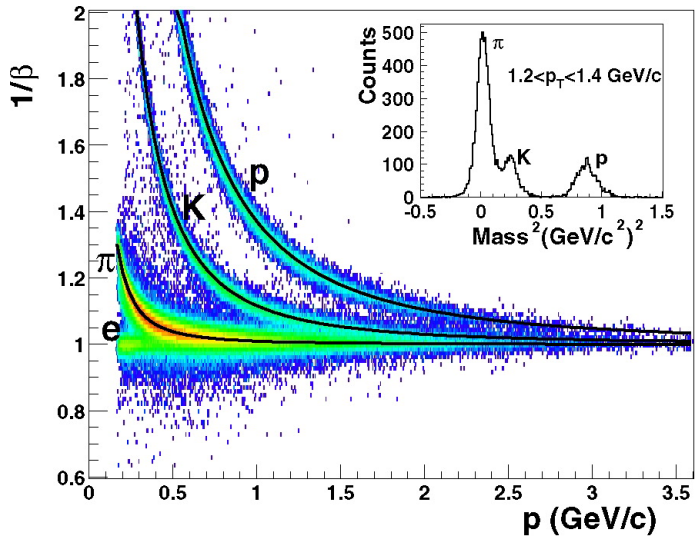

Figure 2.3: Inverse velocity $\frac{1}{\beta}$ for pions π, kaons K and protons p as function of transverse momentum p_T in STAR TOF for d+Au at 200 GeV with projection in range $1,2 < p_T < 1,4$ GeV/c with distinguishable particles. Taken from Ref. [14].

2.3.4 Time Projection Chamber

Time Projection Chamber (TPC) is located between the Heavy Flavor Tracker and the TOF detector. TPC is the main tracking device used for measurements of the trajectories, particles momenta and for particle identification (PID) via ionizing energy loss $\langle \mathrm{d}E/\mathrm{d}x \rangle$. TPC covers the whole azimuth and pseudorapidity $|\eta| \leq 1.8$ [15]. TPC is a barrel shaped with the outer diameter of 4 m and is 4.2 m long filled with the, so called, P10 gas (90% Argon for multiplication and 10 % Methane for quenching). The barrel is divided into 2 parts, the middle membrane is connected to an electric potential of -28 kV and the base is grounded. The area between the membrane and the base is divided into 182 rings, where one ring is common for both halves and carries the membrane. Rings are bridged by 2MΩ resistors providing uniform electric field between the membrane and the base. The scheme of TPC in shown in Figure 2.4.

A charged particle traversing through TPC creates electron–ion pairs. The emitted electrons are drifted towards TPC sides where they are collected. The barrel base is divided into 12 sectors on the basis of Multi–Wire Proportional Chambers(MWPC). Each wire–anode is 20 μm in diameter and provides charge amplification by a factor of 1000–3000. Each sector is divided into 2 halves – inner and outer sector – each with different number of collecting pads.

In year 2019 TPC will be improved to iTPC. TPC transition to iTPC [16] doubles the number of collecting pads front end electronics in the inner sector which improves trajectory reconstruction in pseudorapidity $1 < \eta < 1.8$, enhances the efficiency up to 95 % and improves the measurement of the particle momentum and the energy loss $\langle \mathrm{d}E/\mathrm{d}x \rangle$. By improving the energy loss measurement, one can better distinguish between kaons and protons in the high momentum region [16]. Basic specification of STAR TPC are in Table 2.4.

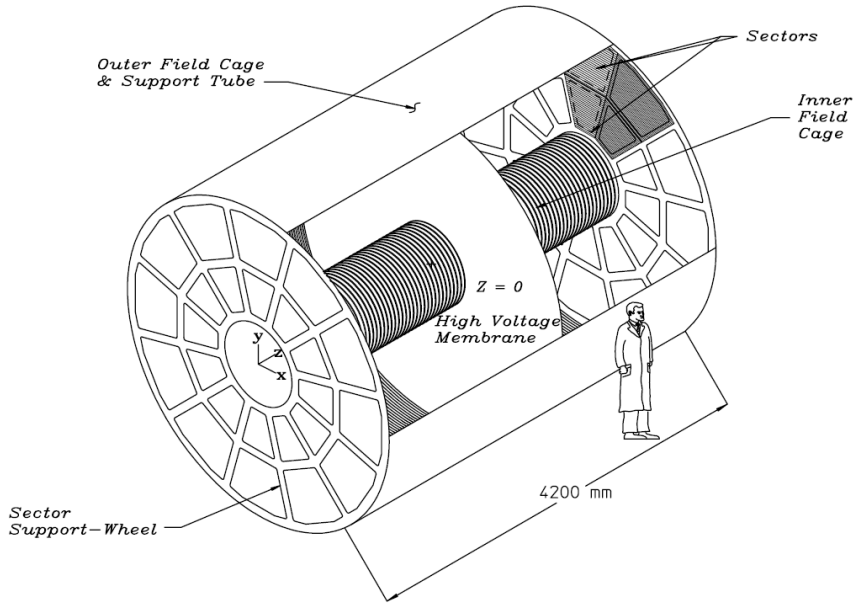

Figure 2.4: Scheme of the STAR TPC. The barrel is divided into two parts by the central membrane (High Voltage Membrane) which is under the potential of -28 kV. The area between the membrane and the base is divided into 182 rings, providing uniform electric field between the membrane and the base. The base is divided into 12 segments used for charge collection. Each segment is divided into inner and outer sector. Taken from Ref. [15].

Charged particles (deuteron, proton, kaon, pion, muon, electron etc.) are identified via ionizing energy loss which obeys the Bethe-Bloch formula [17]

$$-\left\langle \frac{dE}{dx} \right\rangle = 2\pi N_A r_e^2 m_e c^2 \frac{Z}{A}\frac{z^2}{\beta^2}\left[\ln\frac{2m_e c^2\beta^2\gamma^2 W_{max}}{I^2} - 2\beta^2 - \delta(\beta\gamma)\right], \qquad (2.3)$$

where N_A is the Avogadro constant, r_e classical electron radius, m_e electron mass, c speed of light, Z medium atomic number, A medium mass number, z charge of the interacting particle, $\beta = \frac{v}{c}$, where v is the speed of the interacting particle, γ Lorentz factor, I average ionizing energy, δ density correction and W_{max} maximum energy transfer in a single collision.

Energy loss as a function of transverse momentum p_T in STAR TPC is shown in Figure 2.5.

2.3.5 Heavy Flavor Tracker

The inner-most detector of STAR is the Heavy Flavor Tracker (HFT) which is barrel-shaped and consists of 4 layers of silicon detectors. The outermost layer of the HFT is the Silicon Strip Tracker (SST), in the middle Intermediate Silicon Tracker (IST) and the inner–most 2 layers of Pixel detectors (PXL). These detectors improve the tracking and momentum resolution of STAR and are used for more precise measurement of decay vertices. Particle vertex is calculated by fitting hits in detector layers therefore hits closer to vertex greatly enhance fitting resolution.

Outer radius	200 cm
Inner radius	50 cm
Length	420 cm
Pseudorapidity coverage	$\|\eta\| \leq 1.8$
Working gas	P10 (10 % methan + 90 % Argon)
Pressure	atmospheric + 2 mbar
Number of channels	136608
Magnetic field	0.5 T

Table 2.4: Specification of STAR TPC. Taken from Ref. [15].

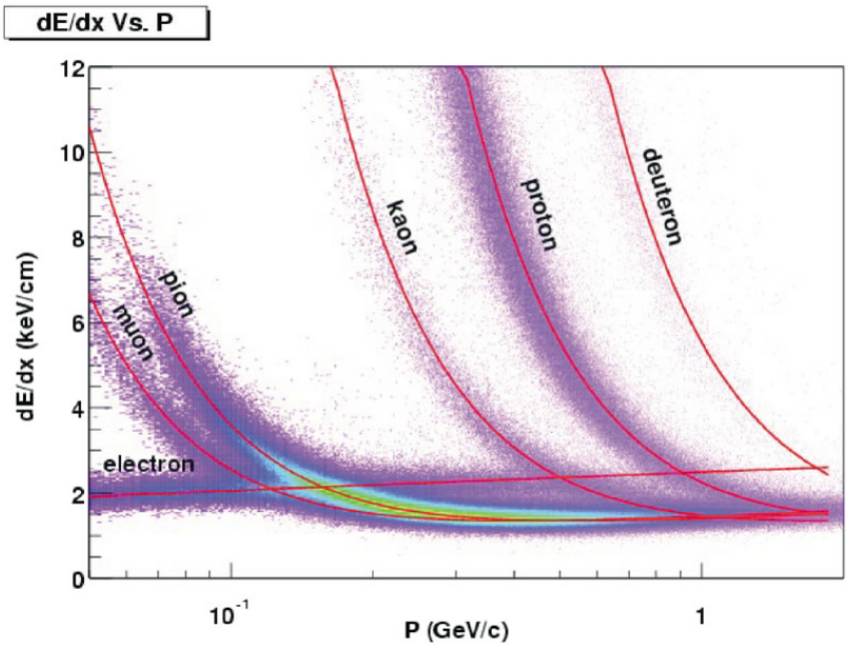

Figure 2.5: Energy loss as a function od transverse momentum p_T with magnetic field 0.25 T. Taken from Ref. [15].

Silicon Strip Tracker

Silicon Strip Tracker is the outermost layer of the HFT, it is barrel–shaped with 22 cm in radius and 106 cm in length, a photograph of the SST can be seen in Figure 2.6. The barrel is divided into 20 triangle cross–sectional ladders carrying 16 double sided strip modules each. Each strip module is 75×42 mm^2 carrying 768 strips of width 95 μm on each side. The Strips enclose the stereoscopic angle of 2°, the total number of channels is 491520. The ladders are air cooled [18]. Basic specification of STAR HFT SST are in Table 2.3.5.

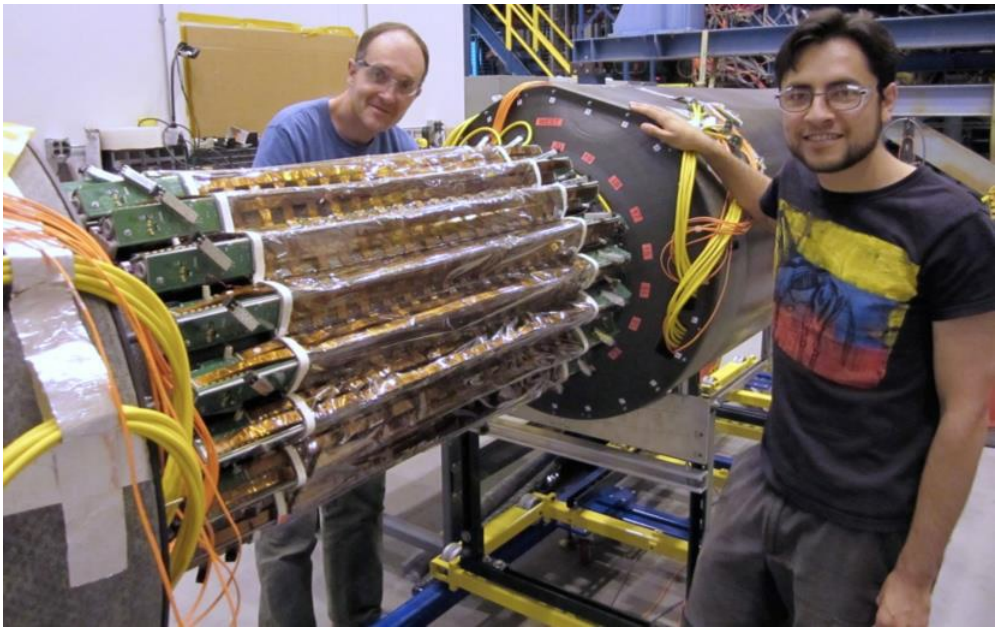

Figure 2.6: SST team installing detector. Taken from Ref. [19].

Radius	22 cm
Length	106 cm
Pseudorapidity coverage	$\|\eta\| \leq 1.2$
Module size	75×42 mm^2
Strip size	73×95 μm^2
R-Φ, Z resolution	740×20 μm^2
Number of channels	4915202

Table 2.5: Specification of STAR SST. Taken from Ref. [18].

Intermediate Silicon Tracker

Intermediate Silicon Tracker makes the second outermost layer of the HFT [18], it is barrel–like with 14 cm in radius and 50 cm in length. Sensors are divided into 24 hybrids (ladders). Each ladder is carrying 6 sensors 76.9×40 mm^2 in size and is divided into 6 chips. Each chip is a strip array of 2 columns and 64 rows, the size of each strip is 6275×596 μm^2. There is a total 110592 strips on 144 sensors, in comparison to SST strips, they are only one–sided. IST covers the pseudorapidity of $-1.2 < \eta < 1.2$ and is cooled by Novec 7200[1] liquid. Photograph of the IST is in the Figure 2.7. Basic specification of STAR IST are in Table 2.3.5.

[1]Novec 7200 during leakage evaporates quickly, does not damage the ozone layer and its vapours are non–flammable and non–toxic.

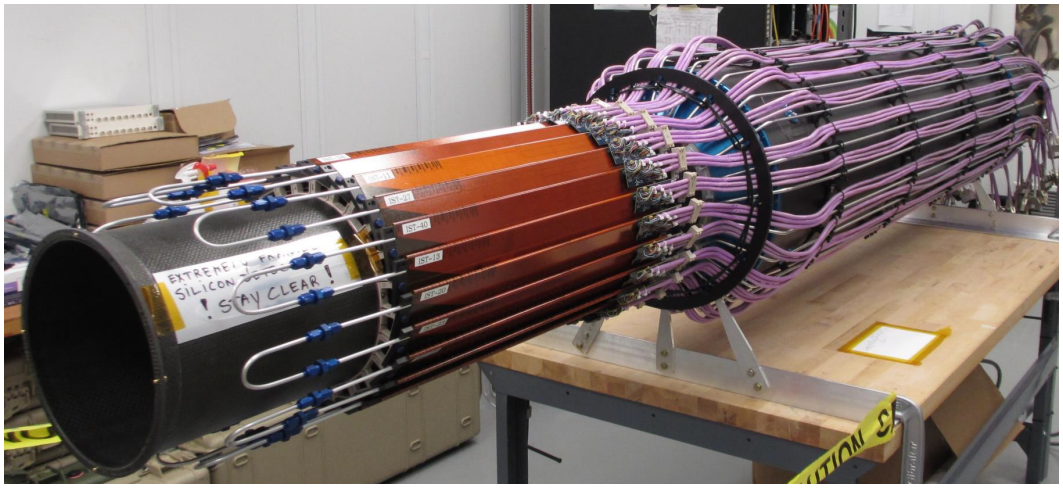

Figure 2.7: IST structure. The ladders are brown, cooling loops on the one side and readout cables on the other side. Taken from Ref. [19].

Radius	14 cm
Length	50 cm
Pseudorapidity coverage	$\|\eta\| \leq 1.2$
Sensor size	76.9×40 mm^2
Strip size	6275×594 μm^2
R-Φ, Z resolution	1811×172 μm^2
Number of channels	110592
Readout time	185.6 μs

Table 2.6: Specification of STAR IST. Taken from Ref. [18, 19].

Pixel detectors

Pixel detectors are the two innermost layers of HFT [18], they are barrel–like with the radii of 2,8 cm and 8 cm. Both layers are attached to a common injection mechanism. The injection mechanism is divided into 10 sectors, each carrying 3 outer pixel ladders and 1 inner pixel ladder. Each ladder has 10 CMOS MAPS sensors of the size 2×2 cm^2. Each sensor is an 960×928 pixel array, with the pixel size of 20.7 μm and thickness of 50 μm. A total of 356M pixels is distributed among the 400 sensors on the 40 ladders. The pixel detector is cooled by air. Due to the proximity to the primary vertex, the sensors must be radiation resilient, because the ionizing environment is $20 - 90$ kRad/year and non–ionizing environment $2 \cdot 10^{11} - 10^{12}$ 1 MeV n eq/cm^2. Thanks to an innovative mechanical injection mechanism, the whole pixel detector can be replaced in one day. Basic specification od HFT PXL is in Table 2.3.5.

Figure 2.8: Structure of the Pixel detector. The sectors are grey and are carrying ladders with detectors, the readout cables are on the far side. Taken from Ref. [19].

Radius	2.8 and 8 cm
Pixel size	20.7×20.7 μm^2
Resolution	< 25 μm
Number of channels	$365M$
Readout time	185.6 μs

Table 2.7: Specification of HFT PXL. Taken from Ref. [18, 19].

2.4 Importance of HFT

Heavy quarks measurements are crucial for heavy ion physics program on RHIC. The main motivation for constructing HFT was to expand the ability of the STAR detector to measure secondary vertices and directly identify particles containing heavy open flavor at p+p, p+A and A+A collisions. Heavy quarks (b, c) are created by hard processes at the beginning of the collision and, during the time evolution, their number is conserved [20]. Thus, they can be used as good QGP probe because they experience the entire evolution of the system. In comparison to light quarks, their yield and lifetime is much smaller thus precise decay vertex detector is needed to select the products of heavy flavor hadrons decay from the combinatorial background.

HFT opens new physics by the measurements of decay vertices by precise measurements of trajectories of the daughter particles, e.g.:

$$D^0 \to K^- + \pi^+,\ c\tau \sim 120\ \mu\text{m},$$

$$D^\pm \to K^\mp \pi^\pm \pi^\pm,\ c\tau \sim 310\ \mu\text{m},$$

$$\Lambda_c^+ \to p + K^- + \pi^+,\ c\tau \sim 60\ \mu\text{m},$$

$$\text{B mesons} \to J/\Psi + X \text{ or } e + X,\ c\tau \sim 500\ \mu\text{m},$$

where $c\tau$ is decay length of particle.

TPC itself has a resolution of 1 mm and each layer of HFT improves it, as can be seen in Figure 2.9. Therefore, decay modes mentioned above can be measured. The distance of closest approach (DCA) resolution can be seen in Figure 2.10

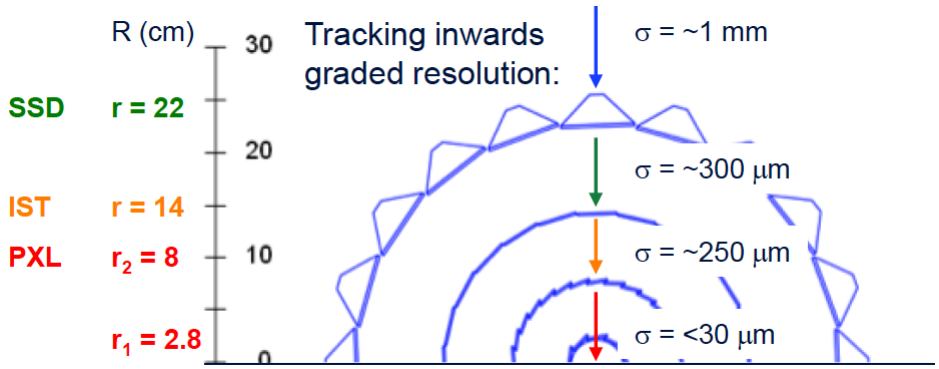

Figure 2.9: DCA resolution for each HFT layer. Taken from Ref. [19].

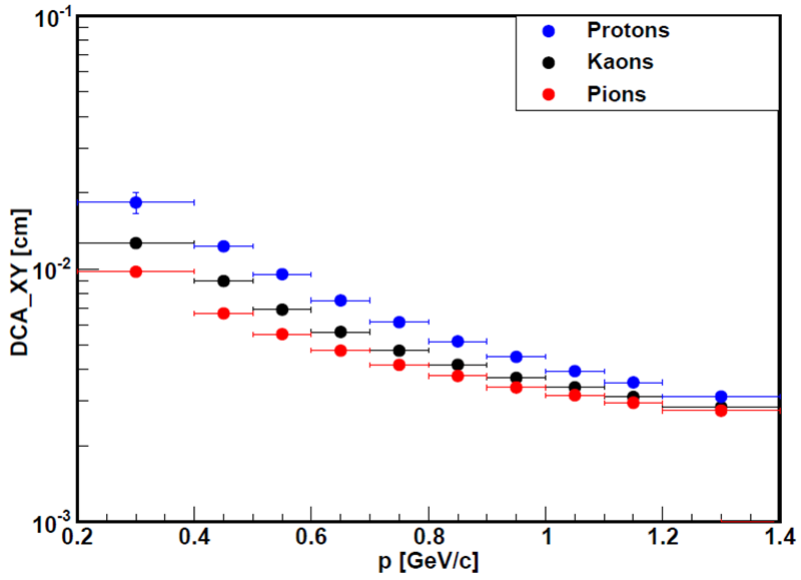

Figure 2.10: DCA resolution with respect to p for protons, kaon and pions. Taken from Ref. [21].

Figure 2.11 shows the D^0 invariant mass measurement. As can be seen in the smaller histogram, without the HFT cuts, no peak can be observed. HFT can suppress the combinatorial background by 4 orders of magnitude.

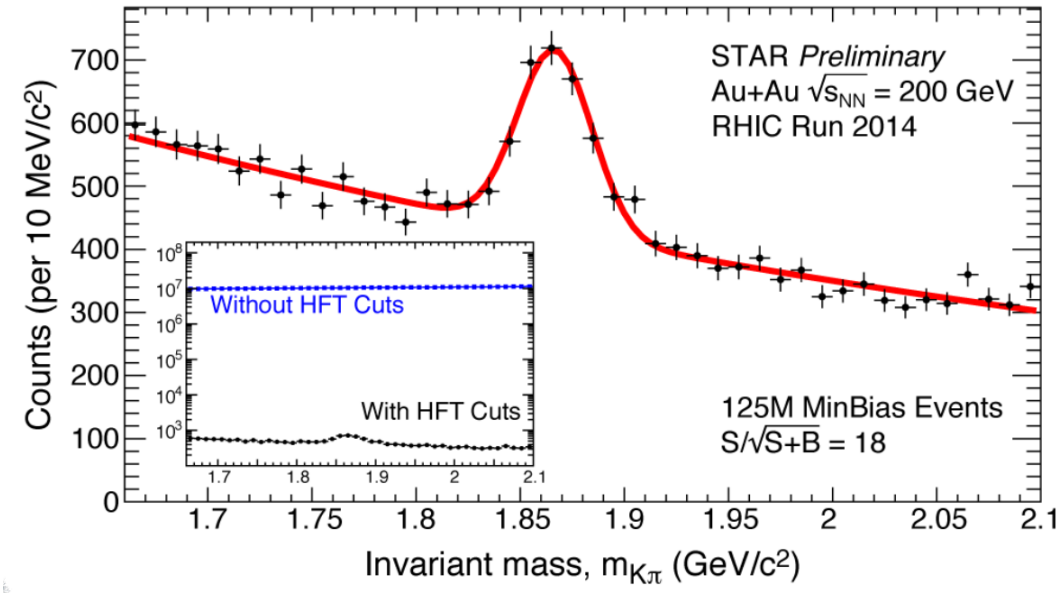

Figure 2.11: D^0 invariant mass for run 2014 Au+Au collisions at $\sqrt{s_{NN}} = 200$ GeV. Smaller histogram shows measurement without HFT cuts (blue points) and with HFT cuts (black points). Taken from Ref. [22].

Chapter 3

HFT pixel simulator

This chapter is dedicated to the first research task of this work – tuning of the pixel detector slow simulator. First, overview in simulation physics and code structure is made. Then, results of cosmic muon calibration is shown and finally, tuning on low luminosity Au+Au data at 200 GeV is described.

3.1 DIGMAPS simulator

Simulations are important for embedding to provide detector efficiency used in particle reconstruction. Basic simulation consists of several steps. First, studied particle is generated, e.g. in PYTHIA, with required particle momentum and is decayed in required channel. The output are particles with various momenta and other kinematics properties. These information enter into GEANT, where passage through each detectors is simulated. Each detector is represented with sensitive volume. These detector signals are reconstructed same as in real collision and detector response and efficiency can be determined [23].

One of the detectors simulated in GEANT is a pixel detector represented by so called fast simulator. Fast simulator takes the hit and smears it by pixel resolution. For more precise simulations a slow simulator for the MAPS sensors at STAR, DIGMAPS, has been developed [24]. In comparison, DIGMAPS can reproduce MAPS sensors' response to the level of a single pixel as well as dE/dx energy deposition in thin silicon, which is approximated by a Lorentzian and a Gaussian. DIGMAPS creates a cluster of pixels to which the random noise is added. This step requires longer computational time compared to the fast simulator. After the DIGMAPS code is implemented into the STAR software, it will replace current pixel simulator in GEANT.

After the DIGMAPS code is implemented into the STAR software, particle trajectories generated by GEANT and the hit positions in the PXL sensor plane will be used as DIGMAPS input. DIGMAPS creates a cluster of pixels to which the random noise is added. After that regular clustering and tracking is done in the same way as during the physical data reconstruction.

In our study, we are using the standalone DIGMAPS tool which generates tracks itself. The reason is we do not need GEANT for cluster generation, thus faster debugging can be done.

3.1.1 Simulation physics

The simulation consists of three steps:

1. particle generation and traversing through the sensor,
2. charge generation and transport,
3. zero suppression and clustering.

First, particle energy deposition: particle is created by MC method and it is traversing through the MAPS sensor. The sensitive area for charged particles in the MAPS sensor is called epitaxial layer with thickness ε, if a generated particle traverses through the sensor – θ is the incident angle to the normal vector to the sensor plane – the effective thickness is equal to $\frac{\varepsilon}{\sin\theta}$. Particle ionizes the material forming electron–hole pairs, the number of pairs is strictly connected to effective thickness. The electron–hole pairs generation obeys the Landau law (PDF: $p(x, MPV, width) = \frac{1}{2\pi i}\int_{c-i\infty}^{c+i\infty} e^{s\cdot y + s\ln s}\mathrm{d}s$, where c is any real positive constant and $y = \frac{x-MPV}{width}$) with MPV 80 e^-/μm and width 18 e^-/μm.

Next, the charge is transported to the collecting N-well diodes which is approximated by the sum of a Gaussian and a Lorentzian thus total charge collected by each pixel can be calculated.

Finally, the zero suppression is performed, based on the ADC threshold level. Clustering in the DIGMAPS standalone tool is done by counting all the hits in the simulated sensor. A graphical representation can be seen in Figure 3.1.

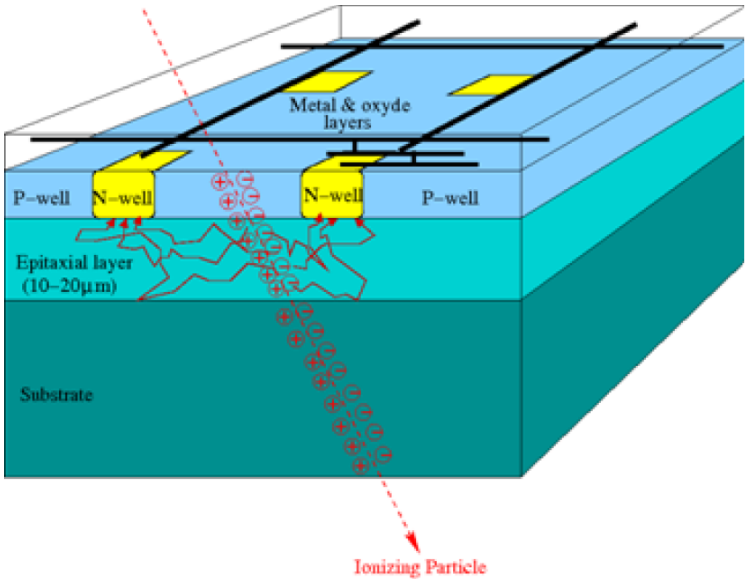

Figure 3.1: A graphical representation of the simulation. Particle ionizes a material forming electron–hole pairs which are collected from the epitaxial layer by N-well diodes. The epitaxial layer thickness was based on an estimate and was not fully calculated in this Figure. The real epitaxial thickness is closer to 9 μm. Taken from Ref. [24].

3.1.2 Standalone DIGMAPS code structure

The DIGMAPS simulator – A standalone software tool to study digitization with MAPS sensor – has been developed in year 2011 at University at Strasbourg.

It is coded in C++ using Root version 5.28 and above. Example of classes

- digmaps.h - Main class that contains pointers to all other classes
- diginitialize.h - Class performing the initialization - reading input data file
- digparticle.h - Class which contain entry and exit point of a particle into the plane, Charge and position of the track, pixel number and charge of collected signal
- digtransport.h - Contains charge transport models
- digadc.h - Contains ADC/discriminator parameters (thresholds. etc.)
- digcluster.h - Contains cluster information (pixel numbers, digital charge)
- digreadoutmap.h - Class containing final output, pixels with collected charge different that 0, analog and digital charge.

Simulation can be run with two commands inside root:

- `.x Run.C`
- `.x Read.C`

Simulator can be compiled by executing `.x Compile.C` command but this is not needed as both Run.C and Read.C script contain compile command.

Run.C link and compile all necessary classes, class examples mentioned above, and creates DIGMAPS type like object. DIGMAPS type object need the name and path of input and output files. Input file includes simulation parameters and output file is .root type file. This step takes seconds for 2000 particles.

Read.C again compiles all classes and creates another DIGMAPS type object. It reads the .root file created in the previous step and creates more histograms in it. This step takes approximately 1 minute for 2000 particles.

I used size of cluster saved in .root file.

Input file

Inside input file several simulation parameters can be set. I used this configuration:

- Theta Incident angle: 0-77.5° (Angle to the normal vector to the sensor plane)
- Phi Incident angle: 0°
- Pixel pitch: 20.7×20.7 μm^2
- Number of pixels: 980×921
- Epitaxial layer thickness 9 μm

- Charge model: 5 (1D Lorentzian+gaussian)
- ADC threshold: 6.2 mV

The pixel pitch and number of pixels are parameters of real pixel sensor used in STAR. The epitaxial layer thickness and charge model are taken from test beam data and ADC threshold is taken from cosmic measurement.

3.2 Cosmic Muon results

The PXL sensors, used in STAR, have a binomial output (either the pixel had a hit or not). Therefore, the only way to compare the simulation to the pixel response to the real particle is by looking at the cluster size. Fortunately, most traversing particles leave a cluster with more than one pixel fired.

Simulator has been compared with signal from cosmic data measurement and ADC threshold has been corrected [25]. In Figure 3.2 is the comparison of simulation for angle 5° with data of incident angle $0 - 10°$. Similar comparison was performed for other angles and ADC thresholds as well. As can be seen in Figure 3.2, the data are consistent with simulation. The DIGMAPS has been tuned for cosmic.

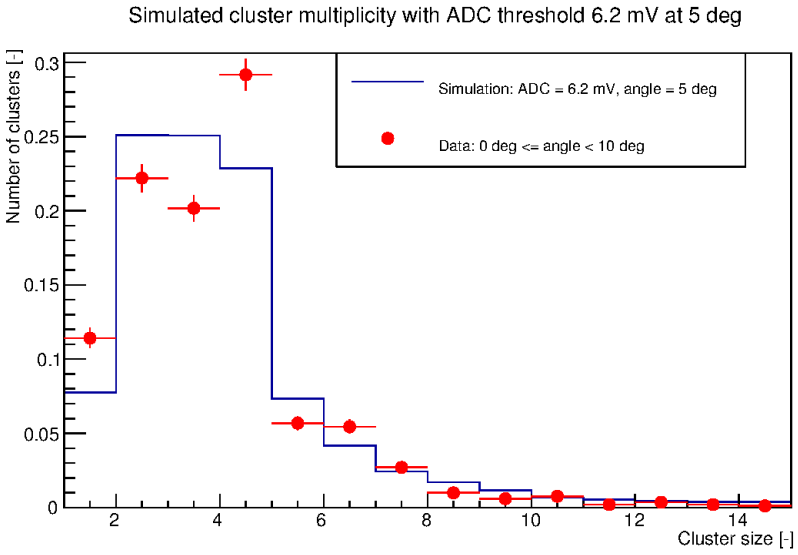

Figure 3.2: DIGMAPS compared to cosmic data at angle $0 - 10°$. [25].

3.3 Low luminosity data testing

For more precise comparison of DIGMAPS to the data, the simulator was tested for all particle species and not only for muons from cosmic radiation. Therefore we have

to use STAR Au+Au low luminosity data[1] at $\sqrt{s_{NN}} = 200$ GeV from year 2014.

3.3.1 Preparation

STAR collaboration uses for analysis reconstructed tracks stored in MuDST[2] and PicoDST files. Within the data reduction during the reconstruction of tracks, we do not store any excessive information. For normal analysis hit information is not required, therefore tracks do not contain information about hits. We need this information in our analysis, therefore we need to do track reconstruction on raw data (containing only hits per event in each detector). I used Au+Au 200 GeV with total 5200 events. For our measurement it is sufficient statistic, as we are analyzing hits in pixel layers and each event provides thousands of hits.

For storing the cluster sizes one needs to add StHftPool class during reconstruction, which identify only Pions for PID, so I have added PID for Kaons and Protons as well.

3.3.2 Selection criteria

Tracks do not contain information about hits, but hits contain information about tracks. Therefore one needs to loop over hits in detectors layers. For each track, we required a hit in the IST layer and both PXL layers in the selected window around the track. I assigned an information about hits to each track, track is discarded if it does not fulfil the bellow mentioned requirements.

The distance between hit and its assigned reconstructed track in a detector plane is called residual distance. Windows for PXL and IST tracks are obtained via fitting of this distributions. The residual distributions for the inner and the outer layer in the x (perpendicular to the beam pipe) and z (longitudinal to the beam pipe) direction of the pixel detector can be seen in Figure 3.3, labelled cuts are taken as 2σ from Gaussian fit.

The exactly one cluster criterion in PXL is used to suppress fake hits caused by random noise in cluster. Furthermore, we used primary tracks only. Primary tracks are the tracks, that originate in primary vertex, i.e. not tracks from secondary decays. All tracks regardless of the origin, i.e. primary and decay vertices tracks, are called global tracks. This assumption greatly reduces the random noise as can be seen in Figure 3.4. After the cuts we did Particle identification (PID).

For PID, we use 2σ energy loss cut in TPC for protons and kaons and 1σ for pions. Cluster size distribution of selected tracks in various p_T and angular interval with corresponding simulation can be seen in Figure 3.4. The summarised cuts can be seen in Table. 3.1

For the total distribution I divided tracks by particle incident degree with 5° step. Then I used DIGMAPS to simulate particles with an incident angle in the

[1] During the charge collection in TPC more collisions may take place, i.e. pileup effect, and one needs to additionally distinguish those events. With higher collision rate – luminosity – the pileup probability is higher, therefore low luminosity data, where pileup effect is suppressed, are used.

[2] Basic data chain is: DAQ→RAW→MuDST→PicoDST. DAQ is the output from detectors itself. RAW is processed DAQ with calibrations and contain hits in each detectors. MuDST contain reconstructed tracks from hits in RAW and PicoDST is more space optimized and contain only most used MuDST informations.

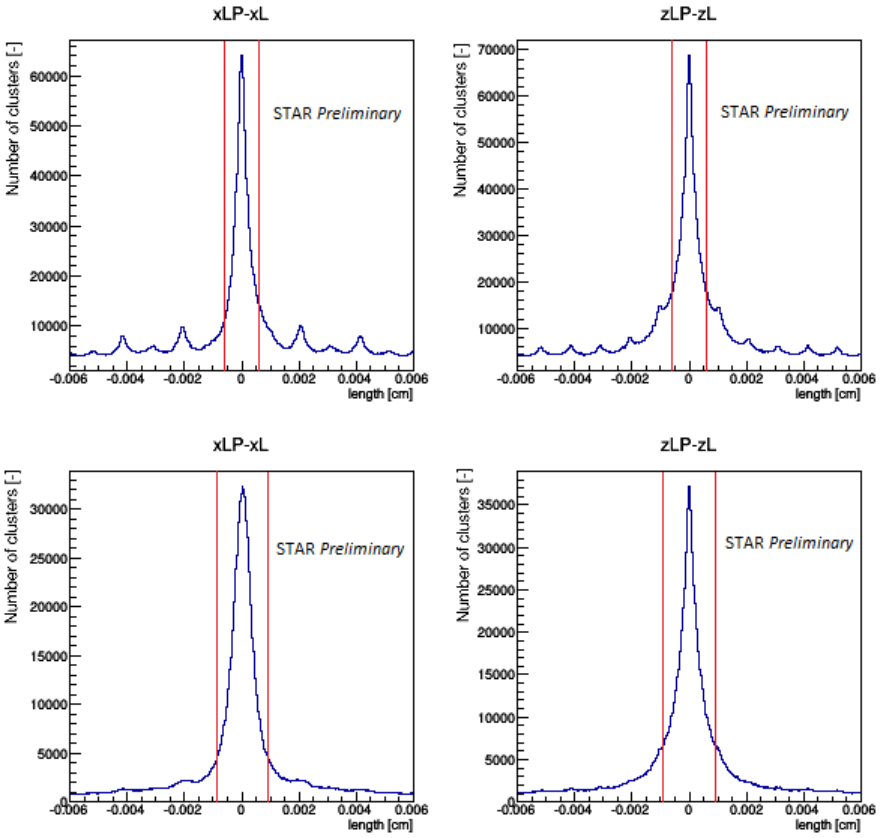

Figure 3.3: Cuts (red) used on residuals for inner (top) and outer (bottom) sensors in x (left) and z (right) plane.

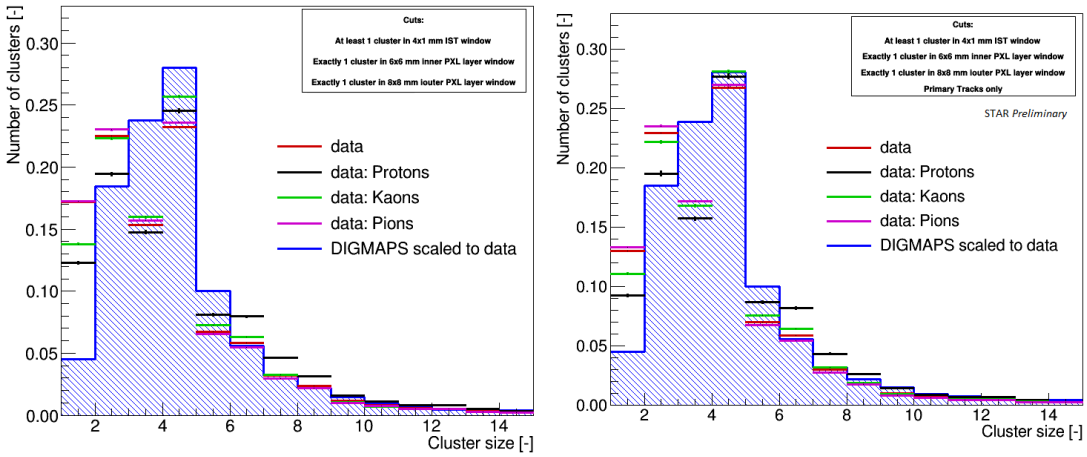

Figure 3.4: Comparison of cluster size of all tracks (left) and primary track only (right).

middle of the interval (the 2.5° incident angle is used for the interval of $0 - 5°$). After this, the simulation output is scaled on data in the corresponding interval for

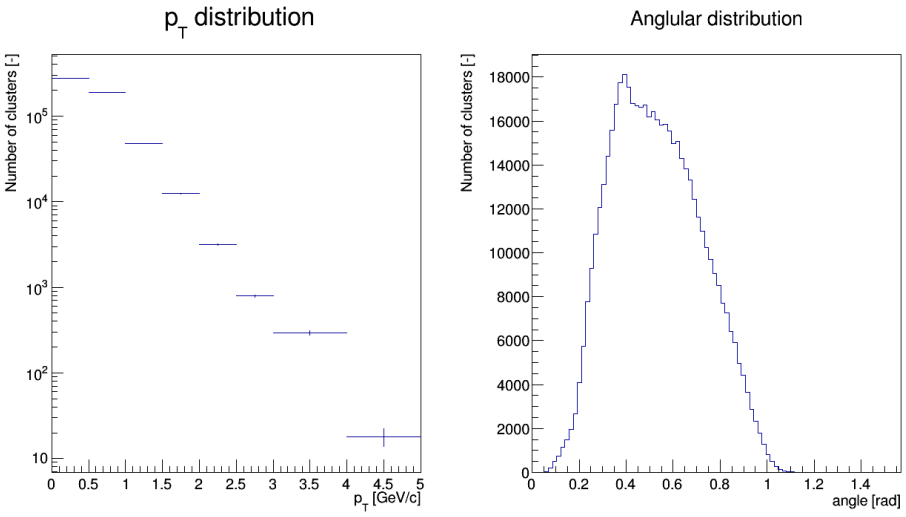

Figure 3.5: p_T and angular distribution of the selected tracks.

a comparison of the shape. This is done for all incident angle intervals and, finally, all scaled results are summed in one output. The results can be seen for example in Figure 3.5 or in Figure 3.6 as blue shaded area.

HFT hits	PXL1, PXL2, IST
max No. hits in each layer	1
IST track window	4×1 mm^2
inner PXL (PXL1) window	6×6 μm^2
outer PXL (PXL2) window	8×8 μm^2
tracks selection	primary only
PID TPC $n\sigma$	p, K: 2σ, π: 1σ

Table 3.1: Data cuts used in DIGMAPS comparison.

3.3.3 Result and discussion

The final result can be seen in Figure 3.6. The data fit the simulation well for high cluster sizes. There is a significant drop for clusters with 3 pixels, which can be seen also in the cosmic data. The cause of this behaviour is currently under investigation.

In Figure 3.7 we compare the DIGMAPS simulation with data for different p_T regions and in Figure 3.8 is DIGMAPS comparison with data for different angle.

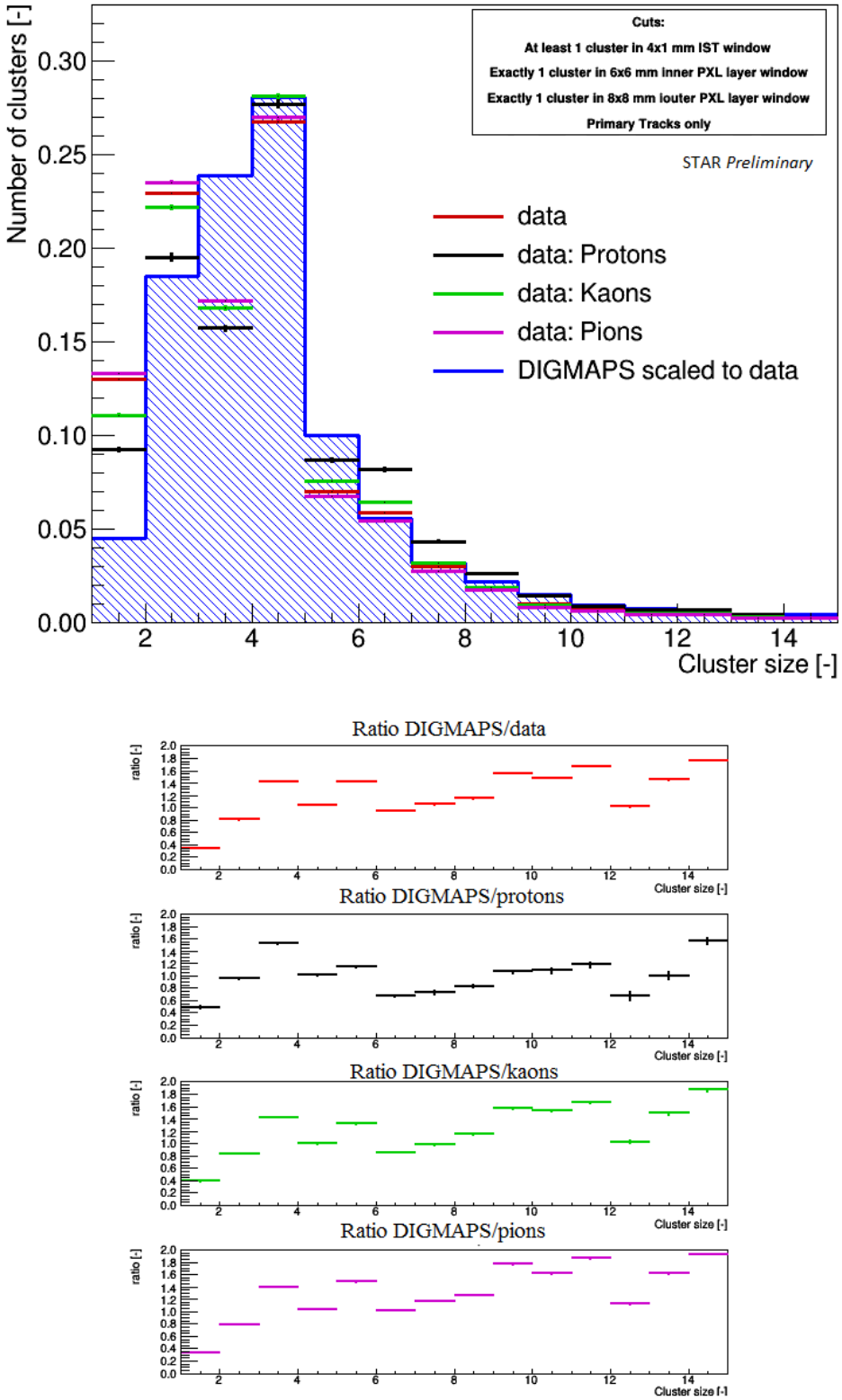

Figure 3.6: DIGMAPS (blue shaded) and low luminosity data comparison. All data (red), protons (black), kaons (green) and pions (magenta). The plot on the bottom shows the ratio for each particle species.

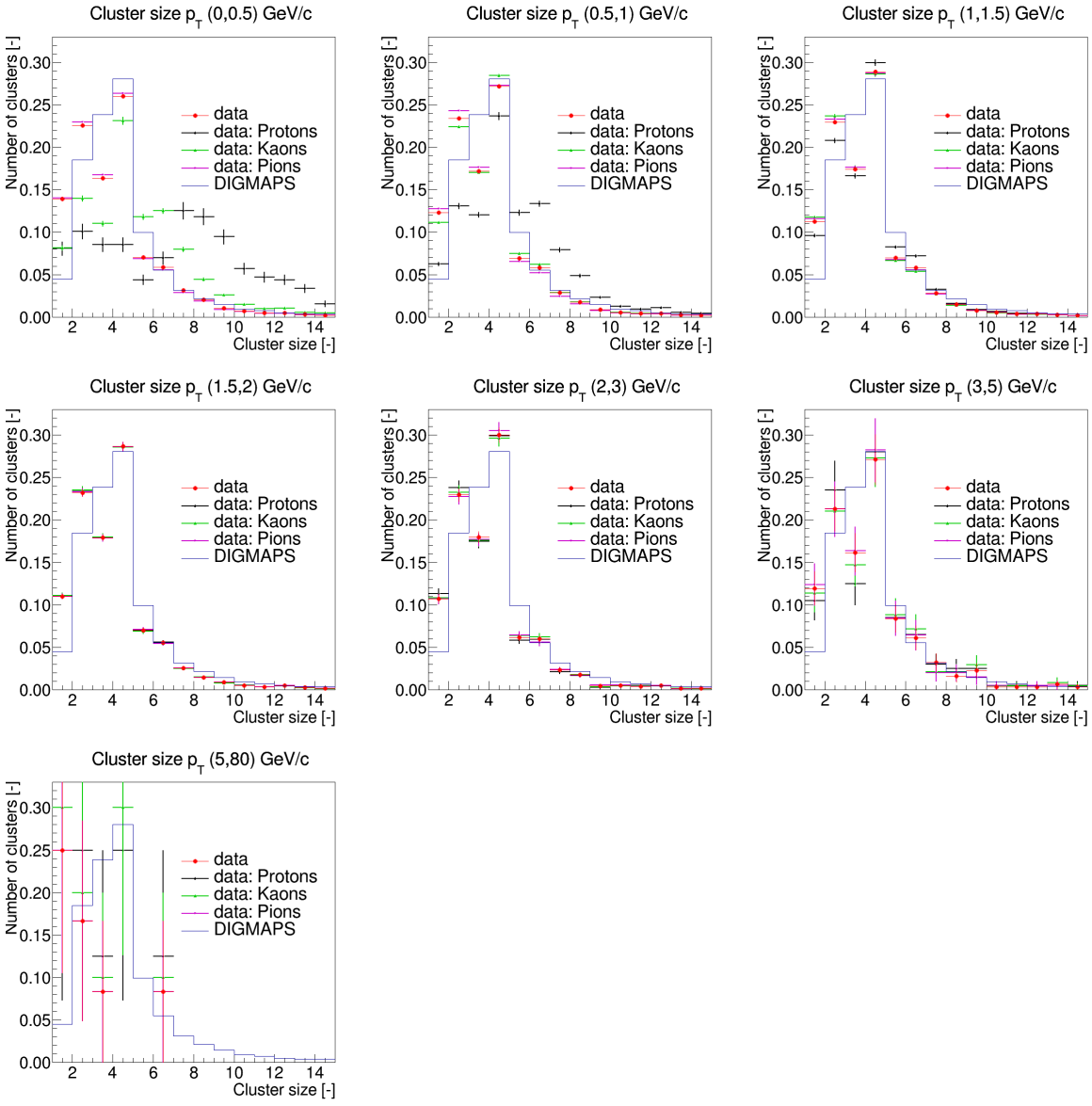

Figure 3.7: DIGMAPS (blue) and low luminosity data comparison for different p_T regions. All particles (red), protons (black), kaons (green) and pions (magenta).

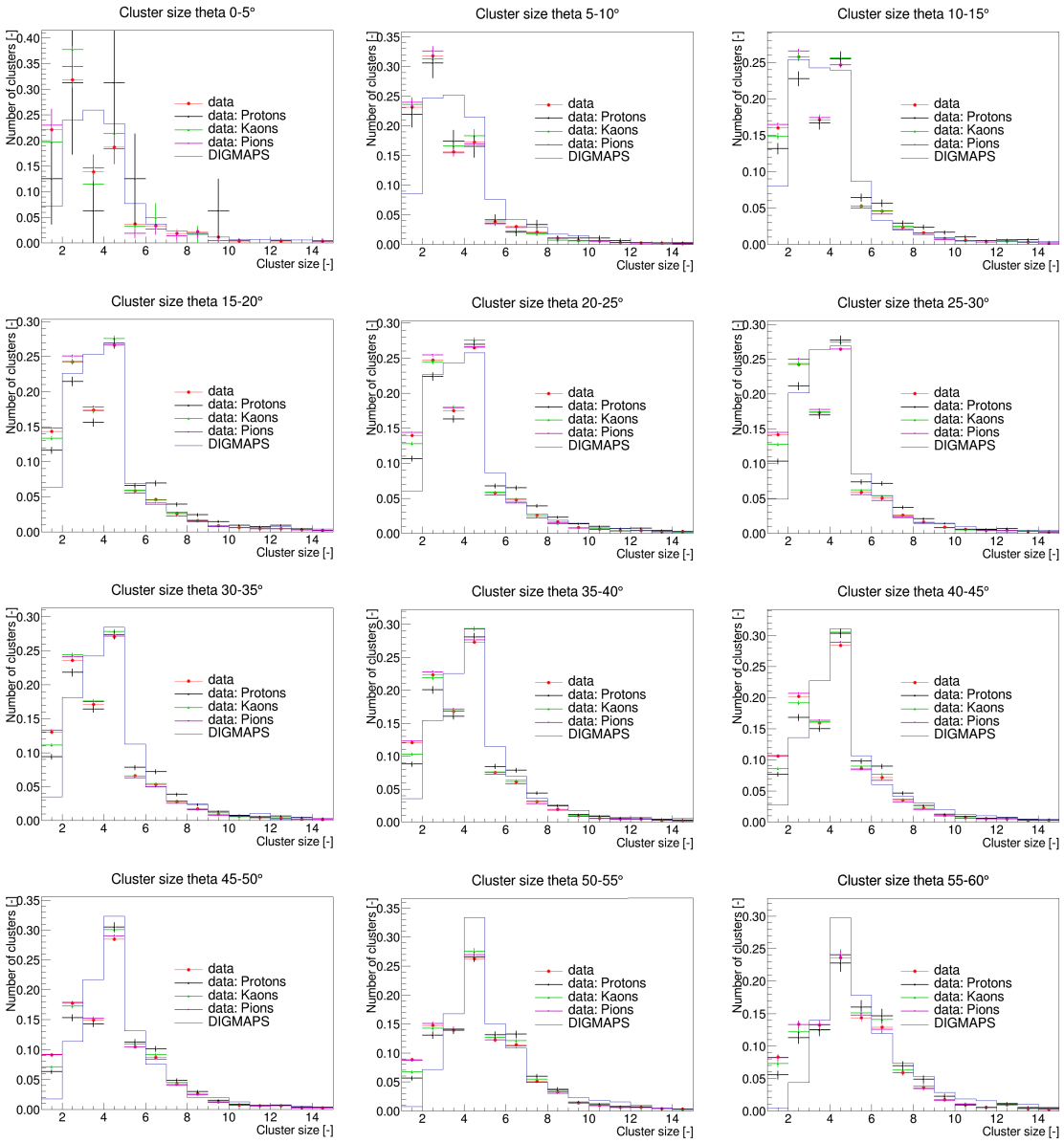

Figure 3.8: DIGMAPS (blue) and low luminosity data comparison for different angle regions. All particles (red), protons (black), kaons (green) and pions (magenta).

Chapter 4

D meson reconstruction

This chapter is dedicated to the second research goal of this work – the $D^{\pm}$ meson reconstruction. In year 2014 STAR collaboration made first attempt to extract $D^{\pm}$ signal [26]. We aim to compare this early results and correct the signal. In the first phase we try to reproduce the results. Basic $D^{\pm}$ properties are shown. The next part describes important cuts that have been made, i.e. event and track selection, particle identification and topological cuts. Finally, invariant mass distribution is shown and subtraction by wrong–correct sign method is made. At the beginning of the year 2016 a software problem, which lower tracking efficiency during HFT reconstruction, was found. Problem has been fixed and a new reconstruction is currently in progress. $D^{\pm}$ reconstruction with this new data can be seen at the end of this chapter.

The fundamental properties of $D^{\pm}$ are shown in the Table 4.1. The D^{+} meson consists of $c\bar{d}$ quark and D^{-} meson of $d\bar{c}$. In this work $D^{\pm}$ are reconstructed directly measuring its decay products, this decay channel has the branching ratio (B.R.) of 9.13%. The $D^{\pm}$ meson decays into $D^{\pm} \rightarrow K^{\mp}\pi^{\pm}\pi^{\pm}$ with the mean decay length is $c\tau = 311.8$ μm, therefore the HFT is necessary in this type of reconstruction to distinguish the D^{+} signal from the combinatorial background of $K\pi\pi$ triplet.

Mass	$m = (1869.61 \pm 0.1)$ MeV/c^2
Mean life time	$\tau = (1040 \pm 7) \times 10^{-15}$ s
Mean flight path	$c\tau = 311.8$ μm
Decay mode	$D^{\pm} \rightarrow K^{\mp}\pi^{\pm}\pi^{\pm}$ B.R 9.13%

Table 4.1: Important $D^{\pm}$ parameters. Taken from Ref. [27].

4.1 Reconstruction of $D^{\pm}$ mesons

4.1.1 Event selection cuts

I used STAR year 2014 AuAu $\sqrt{s_{NN}} = 200$ GeV minimum bias data. Total 1.5 G events has been collected after the trigger restrictions approximately 1.25G events were left. After this, cut on $|v_z(\text{reco.})| < 6$ cm and $|v_z(\text{VPD}) - v_z(\text{reco.})| < 3$ cm has been used where v_z(reco.) is the distance along beampipe from the centre and

v_z(VPD) is the distance along beampipe taken from Vertex Position Detector (VPD). After these two more selection cuts total 1.1G events were accepted. Detailed view can be seen in Figure 4.1.

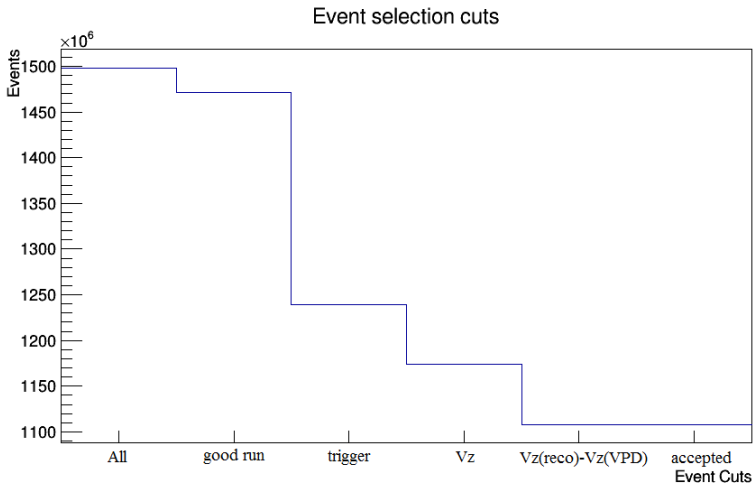

Figure 4.1: Event selection cuts on STAR minimum bias year 2014 AuAu 200 GeV data.

4.1.2 Track selection cuts

Each global track[1] must have hit in each layer of the HFT. That means in both pixel layers, in IST layer and in SST layer. It is also required that the track generated at least 15 hits in TPC.

4.1.3 Particle identification cuts

Several PID cuts have been made. The transverse momentum of pion $p_T^{\pi} > 0.8$ GeV/c and of kaon $p_T^K > 0.6$ GeV/c. TPC $\langle$dE/dx$\rangle$ signal standard deviation for pion and kaon must be smaller then 3σ. Daughters p_T and TPC dE/dx with respect to p_T can be seen in Figure 4.4.

The transverse momentum from TOF of pion $p_{T_{TOF}}^{\pi} > 0.2$ GeV/c and of kaon $p_{T_{TOF}}^{K} > 0.2$ GeV. The inverse pion velicity $|\frac{1}{\beta} - \frac{1}{\beta_\pi}| < 0.05$ and kaon $|\frac{1}{\beta} - \frac{1}{\beta_K}| < 0.06$, where $\frac{1}{\beta_X}$ is inverse velocity of track calculated from track momentum and tabular particle X mass and $\frac{1}{\beta}$ is measured inverse velocity of track from TOF detector.

4.1.4 Topological cuts

At this point, each event are investigated for D$^{\pm}$ candidates, thus topological cuts in vertex reconstruction are applied. The distance of closest approach (DCA) between daughter pair tracks ($\pi\pi$, πK, $K\pi$) must be smaller than 80 μm. The distance of

[1] All tracks regardless of the origin, i.e. primary and decay vertices tracks, are called global tracks. Primary tracks are the tracks, that originate in primary vertex, i.e. not tracks from secondary decays.

reconstructed vertex from primary vertex (in other words, reconstructed $D^{\pm}$ mean decay length) must be greater than 30 μm and smaller than 2000 μm. The lower limit is taken from PXL minimum resolution to distinguish between primary and secondary vertices. The pointing angle $\cos\theta$ must be greater than 0.998. The pointing angle is the deviation between the reconstructed momentum direction of $D^{\pm}$ and primary vertex as can be seen in Figure 4.2.

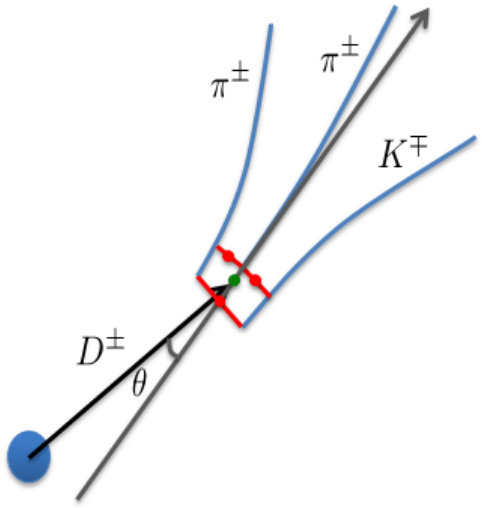

Figure 4.2: The $D^{\pm}$ pointing angle. Its the deviation of the reconstructed momentum vector and primary vertex. Taken from Ref. [26].

With these cuts and PID cuts discussed above, approximately 150M candidate triplets were selected. Another cut on $\Delta_{max} < 200$ μm has been made. Δ_{max} is the maximum distance between $v_{\pi\pi}$, $v_{\pi K}$ and $v_{K\pi}$, where $v_{\pi K}$ is the reconstructed vertex of π and K etc. The Δ_{max} cut can be seen in Figure 4.5. The daughter DCA to primary vertex must be greater than 100 μm for pions and 80 μm for kaons to be certain they do not originate from primary vertex, total 27k candidate triplets passed, DCA distribution for pions and kaon can be seen in Figure 4.4. Candidate triplets divided by charge combination can be seen in Figure 4.3. That means the first bin represent the D^{+}, second bin D^{-} and the rest are different wrong charge combination used as wrong–sign background.

All used cuts are summarised in the Table 4.2.

4.2 Wrong–sign background and Yield

After applying cuts and constructing invariant mass from conservation of four–momentum, the signal of $D^{\pm}$ can be seen in Figure 4.6 and the p_T distribution of this signal can be seen in Figure 4.7. As a background estimation wrong sign–correct sign method has been used. The background has been created as wrong charge combination according to Figure 4.3 and can be seen in Figure 4.6.

The signal peak in Figure 4.6 was fitted with a Gaussian and 3σ wide windows

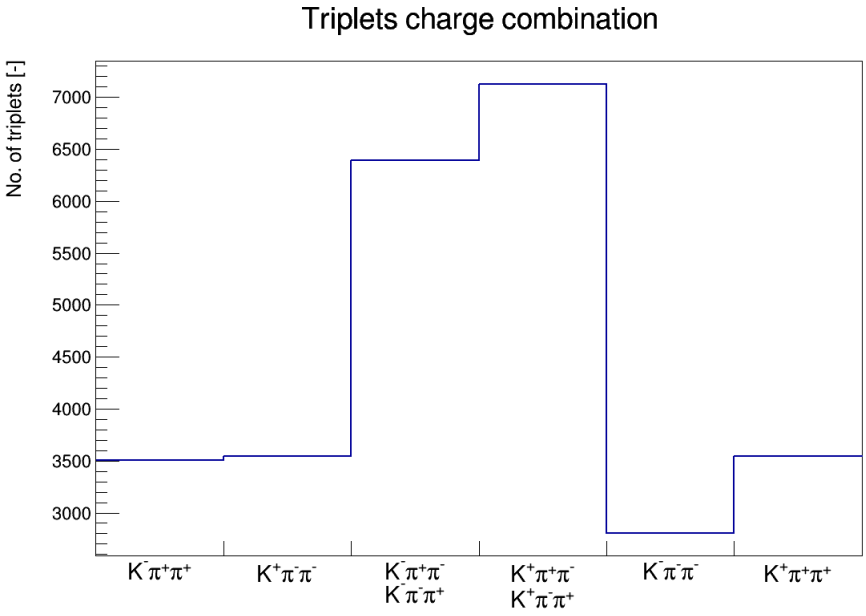

Figure 4.3: The $D^{\pm}$ candidate triplets charge combinations. The first bin represents the D^{+}, second bin D^{-} and the rest are different wrong charge combination used as wrong sign–correct sign background.

were used as a signal interval, i.e. $(1.795 - 1.945)$ GeV/c^2. Counts outside signal interval were counted and simultaneously, counts outside same interval were counted in background, thus the scaling parameter has been estimated. The background was scaled and subtracted from signal+background, the result can be seen in Figure 4.8.

As can be seen, significant residual background remains so the following correction was applied: The signal has been fitted with a Gaussian and a Polynomial of the first order and the Polynomial has been subtracted. Corrected invariant $D^{\pm}$ mass distribution can be seen in Figure 4.9. The peak has been fitted with a Gaussian and the invariant mass has been estimated as $m_{D^{\pm}} = (1.87 \pm 0.03)$ GeV/c^2, in this range, yield has been determined as 330±50 with a signal significance 6.9σ. The significance has been evaluated as $\sqrt{\frac{S}{S+2B}}$, where S is the signal part of a peak and B is the background part of a peak.

I used cuts [26] with slightly modification, I have added the TOF pion restrictions $|\frac{1}{\beta} - \frac{1}{\beta_\pi}| < 0.05$ and $p_T^{\pi} > 0.2$. The first reproduction of $D^{\pm}$ from year 2014 can be seen in Figure 4.10. More restrictive cuts on $D^{\pm}$ momentum and collision centrality were used. Nevertheless the yield is similar.

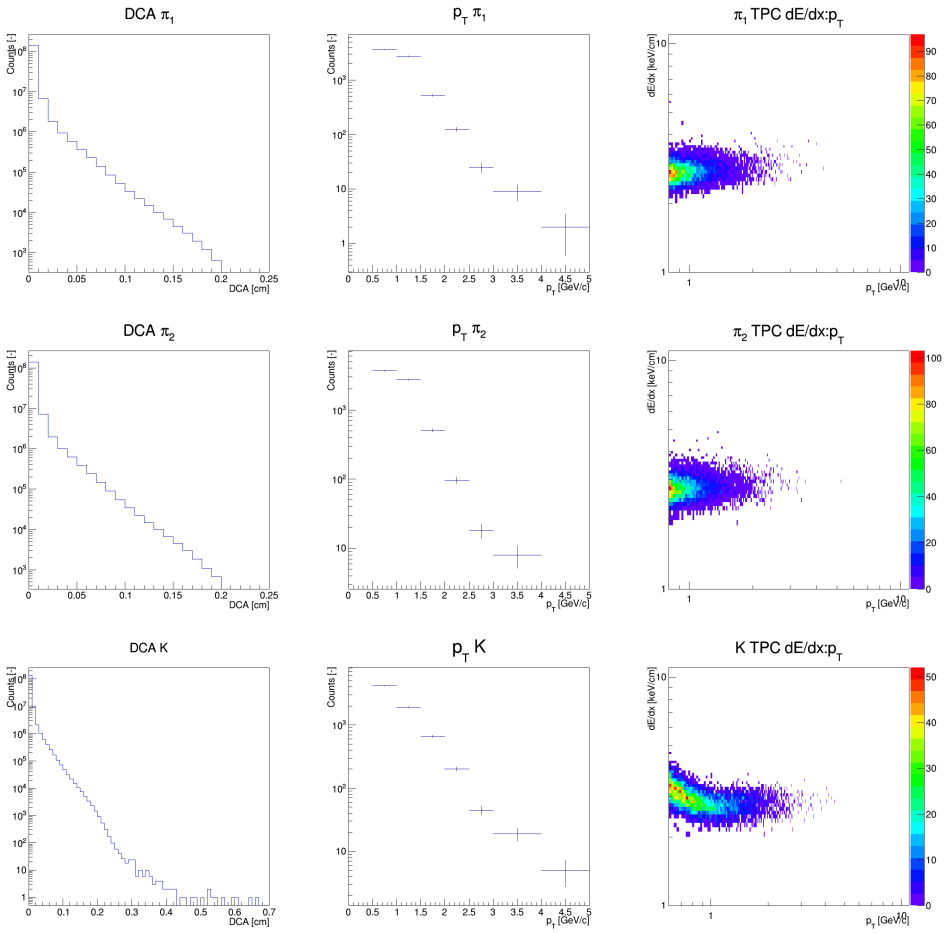

Figure 4.4: Left: The Distance of closest approach (DCA) for π_1, π_2 and K. Middle: p_T for π_1, π_2 and K. Right: TPC ionizing loss for π_1, π_2 and K.

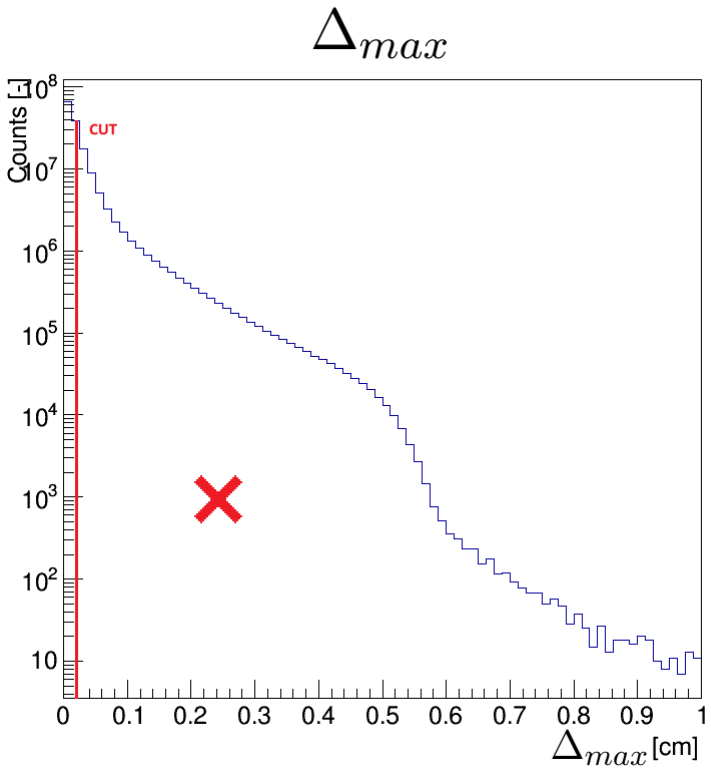

Figure 4.5: The cut on Δ_{max}. Δ_{max} is the maximum distance between $v_{\pi\pi}$, $v_{\pi K}$ and $v_{K\pi}$, where $v_{\pi K}$ is the reconstructed vertex of π and K etc.

Event selection	Distance along beampipe	$\|V_z(reco.)\| < 6$
	Deviation between VPD and distance	$\|V_z(VPD) - V_z(reco.)\| < 3$
Track selection	Hits HFT	PXL1, PXL2, IST, SST
	Hits in TPC	$N_{TPC} > 15$
Topological Cuts	DCA between $\pi\pi$, πK, $K\pi$	$DCA_{XY} < 80$ μm
	$D^{\pm}$ mean flight path	30 μm $< c\tau <$ 2000 μm
	Pointing angle	$\cos\theta > 0.998$
	Max reconstructed vertex pair distance	$\Delta_{max} < 200$ μm
	Daughter DCA to primary vertex	$DCA_{\pi 0} > 100$ μm
		$DCA_{K0} > 80$ μm
Particle identification	TPC particle transverse momentum	$p_T^{\pi} > 0.8$ GeV/c
		$p_T^{K} > 0.6$ GeV/c
	TPC ionization loss standard deviation	$n\sigma_{\pi} < 3$
		$n\sigma_{K} < 3$
	TOF particle transverse momentum	$p_T^{\pi} > 0.2$ GeV/c
		$p_T^{K} > 0.2$ GeV/c
	TOF inverse velocity	$\|\frac{1}{\beta} - \frac{1}{\beta_{\pi}}\| < 0.05$
		$\|\frac{1}{\beta} - \frac{1}{\beta_{K}}\| < 0.06$

Table 4.2: Summary of used event selection, track selection, topological cuts and PID cuts. Taken from Ref. [28] and modified.

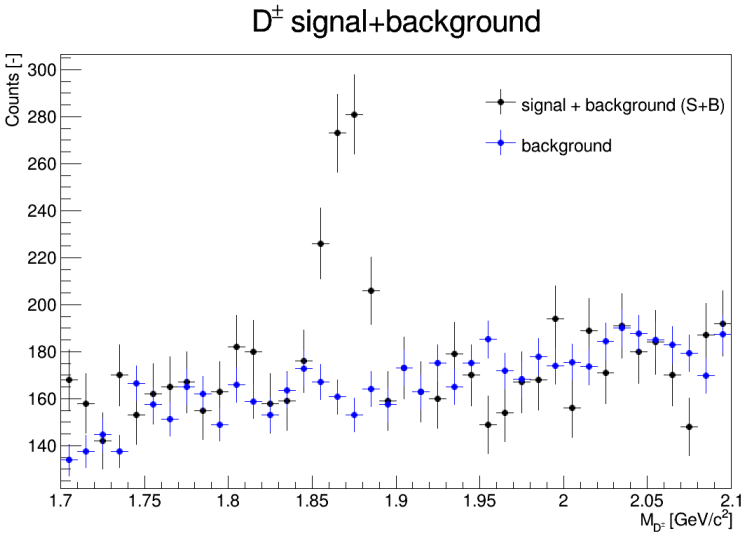

Figure 4.6: The $D^{\pm}$ signal+background for Au+Au $\sqrt{S_{NN}} = 200$ GeV.

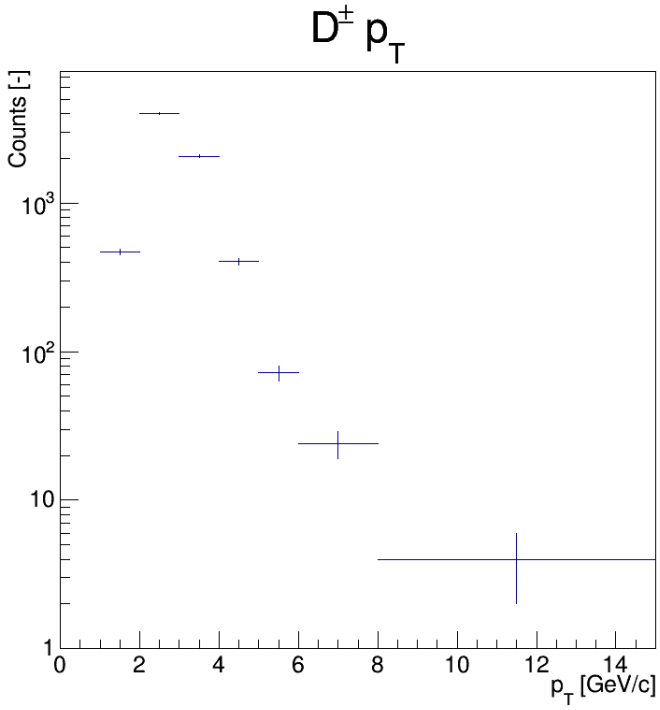

Figure 4.7: p_T distribution of signal+background $D^{\pm}$ distribution.

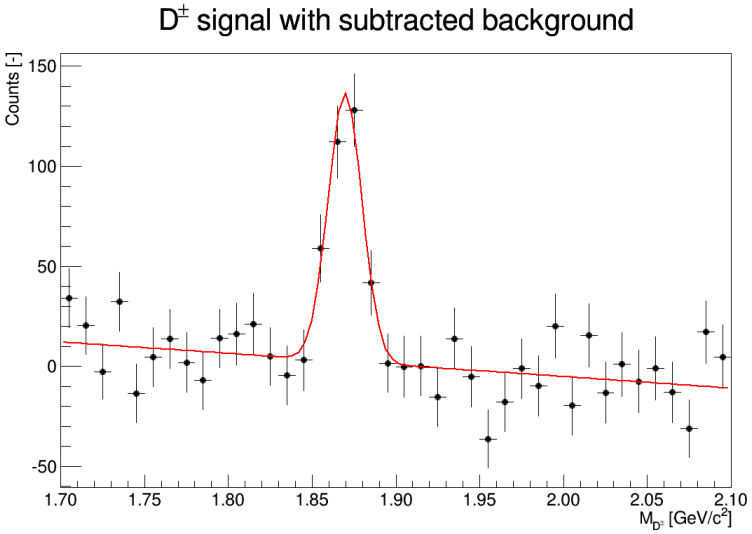

Figure 4.8: The $D^{\pm}$ signal after background subtraction.

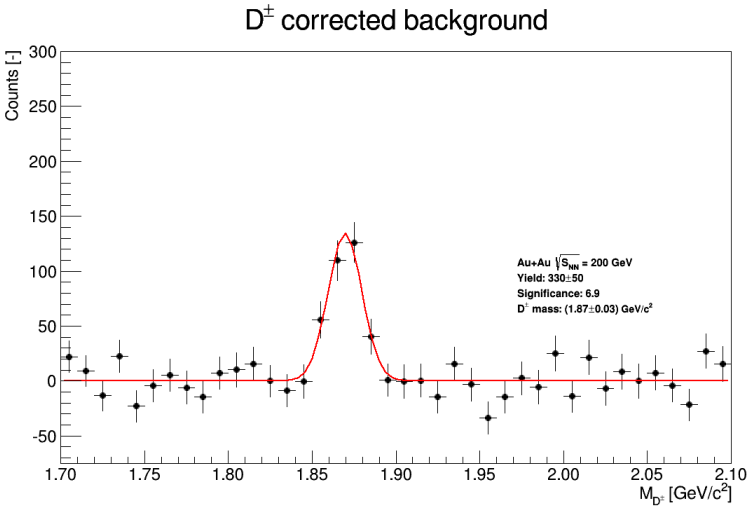

Figure 4.9: The $D^{\pm}$ signal after background subtraction and linear correction.

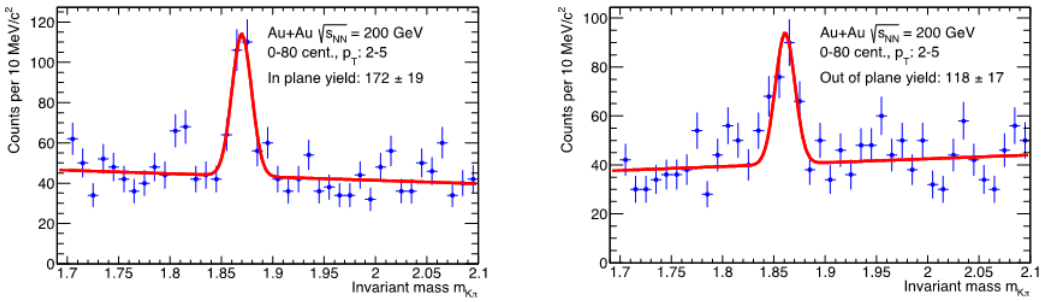

Figure 4.10: The $D^{\pm}$ signal and yield. Taken from Ref. [26].

4.3 Reconstruction of $D^{\pm}$ mesons with fixed MuDST reconstruction software

At the beginning of the year 2016 a software problem, which lower tracking efficiency during HFT reconstruction, was found. Problem has been fixed and a new reconstruction is currently in progress. Already 150M events was reconstructed and analyzed with same cuts mentioned in Table 4.2.

Detailed view on events after event selection cuts can be seen in Figure 4.11. Candidate triplets divided by charge combination can be seen in Figure 4.12. First bin represent the D^{+}, second bin D^{-} and the rest are different wrong charge combination used as wrong–sign background.

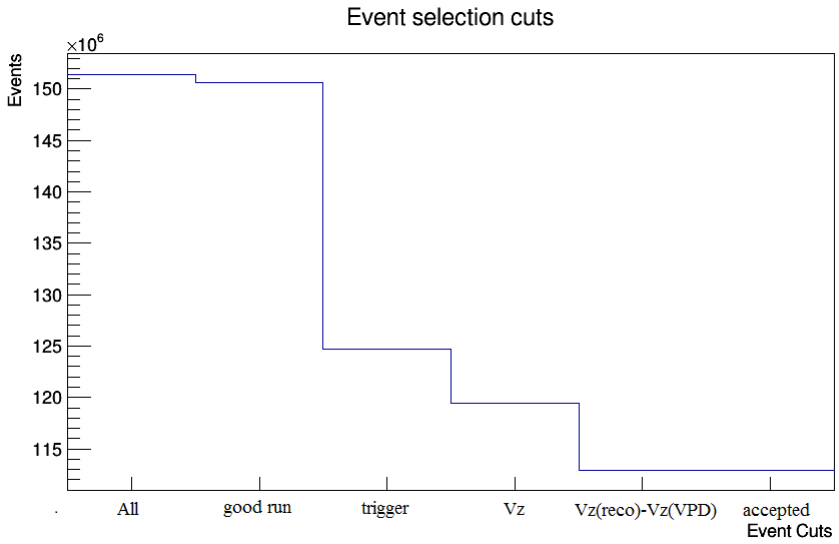

Figure 4.11: Event selection cuts on STAR minimum bias year 2014 AuAu 200 GeV new reproduction data with fixed reconstruction software.

The signal of $D^{\pm}$ can be seen in Figure 4.13. As a background estimation wrong sign–correct sign method has been used. The background has been created as wrong charge combination according to Figure 4.12 and can be seen in Figure 4.13. After background and residual background subtraction, the invariant $D^{\pm}$ mass distribution can be seen in Figure 4.14. The peak has been fitted with a Gaussian and the invariant mass has been estimated as $m_{D^{\pm}} = (1.87 \pm 0.03)$ GeV/c^2, in this range, yield has been determined as 830±50 with a signal significance 17.7σ. The significance has been evaluated as $\sqrt{\frac{S}{S+2B}}$, where S is the signal part of a peak and B is the background part of a peak. Owing to great peak significance the signal has been divided into different p_T intervals and can be seen in Figure 4.15. There is no peak in the first region due to track selection cuts and the significance in the rest intervals is immense and p_T intervals can be further split.

The Yield is almost 3× greater than in previous reconstruction, however the analysis was done on 10× smaller statistic, therefore the enhancement is really remarkable. The peak significance almost triples to 17.7σ and the background off the peak is slightly smaller. Looking on full statistics will be very interesting.

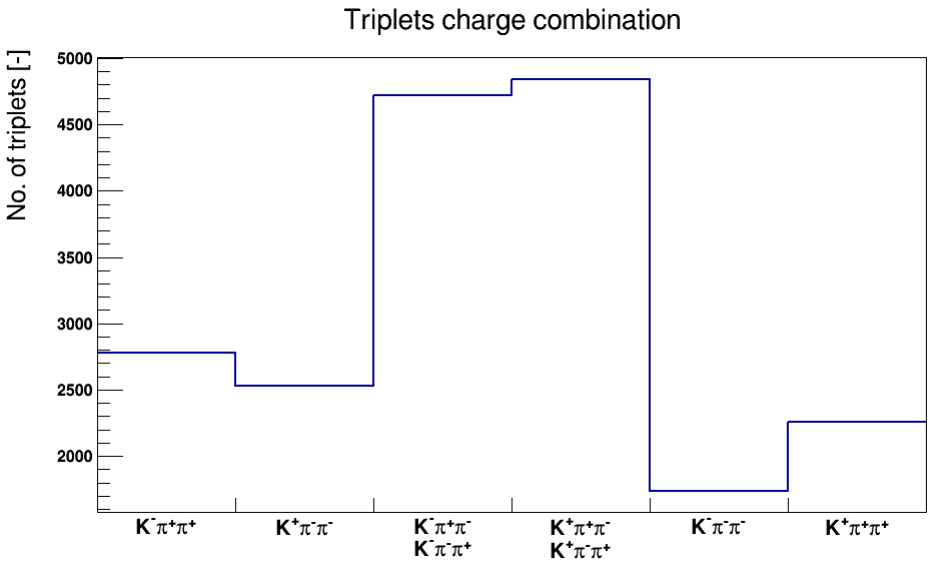

Figure 4.12: The D$^{\pm}$ candidate triplets charge combinations with fixed reconstruction software. The first bin represents the D^{+}, second bin D^{-} and the rest are different wrong charge combination used as wrong sign–correct sign background.

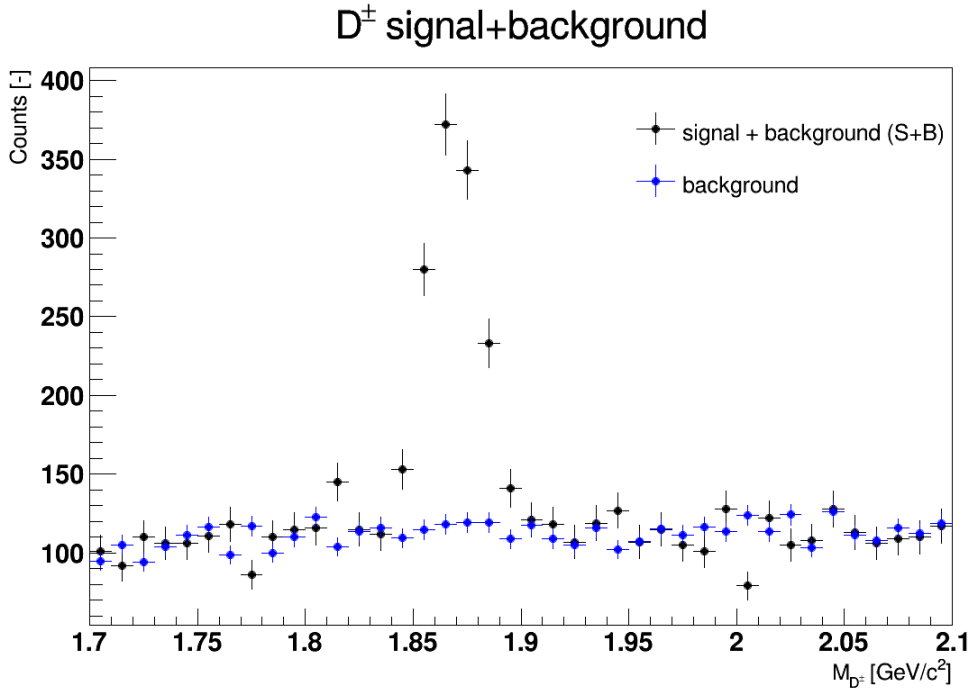

Figure 4.13: The D$^{\pm}$ signal+background for Au+Au $\sqrt{S_{NN}}$ = 200 GeV data with fixed reconstruction software.

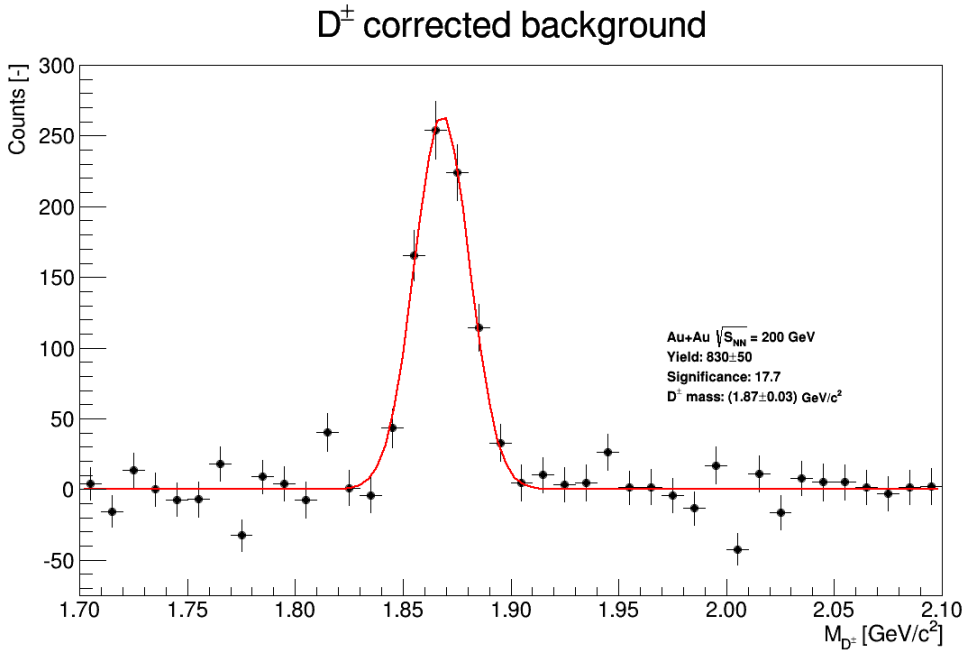

Figure 4.14: The $D^{\pm}$ signal, with fixed reconstruction software, after background subtraction and linear correction.

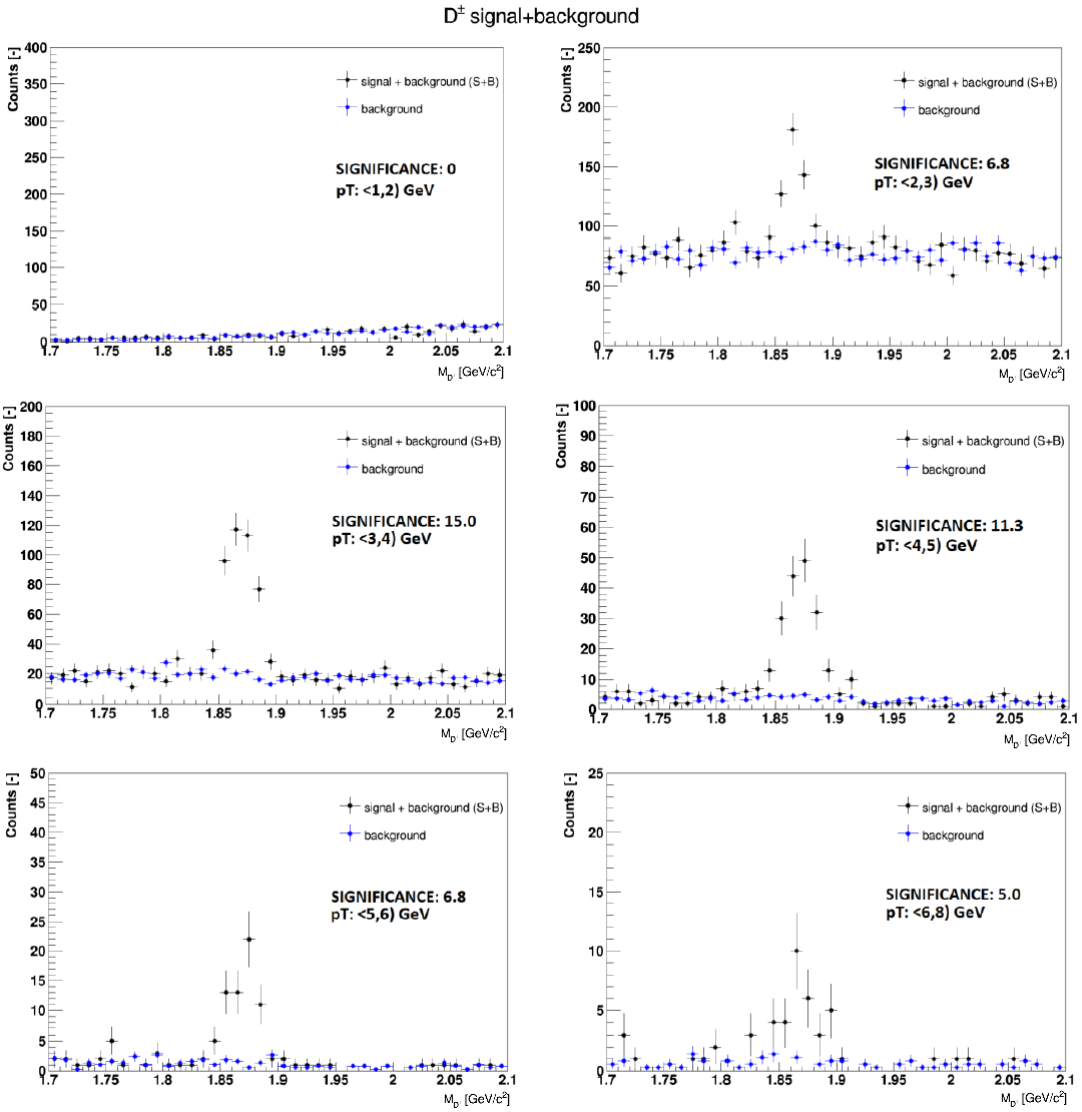

Figure 4.15: The D± signal, with fixed reconstruction software, divided in different p_T bins.

Chapter 5

Summary

The Heavy Flavor Tracker provides an excellent tool for measurements of the heavy flavor hadrons via precise measurements of the decay vertices. Heavy quarks (b,c) are created in hard processes at the beginning of collision thus experience the whole evolution of the hot and dense nuclear matter and can act as a good probe to the physical properties of the strongly interacting quark-gluon plasma.

First, to improve simulations, which are important for embedding to provide detector efficiency used in particle reconstruction, a slow simulator called DIGMAPS has been developed. DIGMAPS has been tested and tuned on cosmic muon data. More tuning was made with the year 2014 Au+Au $\sqrt{s_{\mathrm{NN}}} = 200$ GeV low luminosity data and the results are satisfying.

Furthermore, direct reconstruction of $\mathrm{D}^{\pm}$ meson signal has been made on run 2014 Au+Au data at $\sqrt{s_{\mathrm{NN}}} = 200$ GeV. This measurement is possible because of the sufficient tracking resolution provided by HFT. This is also one of the first $\mathrm{D}^{\pm}$ measurement made at RHIC. Finally, the invariant mass distribution has been evaluated with subtracted background by wrong–sign method. The invariant mass has been estimated as (1.87 ± 0.03) GeV with peak significance 6.9σ.

A remarkable improvement to the HFT efficiency was achieved by a software upgrade. With new reconstruction the peak significance enhanced up to 17.7σ. The analysis was done on $10\times$ smaller statistic.

The next steps of this analysis are to optimize the selection criteria for signal by multivariate analysis, make corrections for detector geometric acceptance and reconstruction efficiency, evaluate $\mathrm{D}^{\pm}$ spectra, ratio between D^{0} and $\mathrm{D}^{\pm}$ and nuclear modification factor R_{AA}.

List of abbreviation

AGS ..... Alternating Gradient Synchrotron

BEMC ..... Barrel Electromagnetic Calorimeter

BNL ..... Brookhaven National Laboratory

CBM ..... Compressed Baryonic Matter experiment

CMOS ..... Complementary Metal Oxide Semiconductor

DAQ ..... Data acquisition

EBIS ..... Electron Beam Ion Source

eRHIC ..... The electron Relativistic Heavy Ion Collider

FAIR ..... Facility for Antiproton and Ion Research

HFT ..... Heavy Flavor Tracker

IST ..... Intermediate Silicon Tracker

LHC ..... The Large Hadron Collider

Linac ..... Linear accelerator

MAPS ..... Monolithic Active Pixel Sensor

MRPC ..... Multigap Resistive Plate Chambers

MTD ..... Muon Telescope Detector

MWPC ..... Multi-Wire Proportional Chambers

pVPD ..... Vertex Position Detector

PXL ..... Pixel detector

RHIC ..... The Relativistic Heavy Ion Collider

RHICf ..... RHIC forward

SST ..... Silicon Strip Tracker

STAR ..... Solenoidal Tracker At RHIC

TOF ..... Time of Flight

TPC ..... Time Projection Chamber

VPD ..... Vertex Position Detector

Bibliography

[1] Brookhaven National Laboratory, *The Relativistic Heavy Ion Collider* [Web],cit. 27.4.2015 http://www.bnl.gov/rhic/default.asp.

[2] Wolfram Fischer, *Run overview of the Relativistic Heavy Ion Collider*[WEB],cit. 27.4.2015 http://www.rhichome.bnl.gov/RHIC/Runs/.

[3] Karen McNulty Walsh, *Accelerating Particles Accelerates Science — With Big Benefits for Society*[Obrázek], http://www.bnl.gov/rhic/news2/news.asp?a=3758&t=today.

[4] W. Fisher, J. Alessi, M. Blaskiewicz, et al., *RHIC Collider Projections (FY 2016 - FY 2022)*[Online],cit. 28.6.2015 http://www.rhichome.bnl.gov/RHIC/Runs/RhicProjections.pdf.

[5] H. Hahn, E. Forsyth, H. Foelsche, et al., *The RHIC design overview*, Nucl.Instrum.Meth., vol. A499, pp. 245–263, 2003.

[6] The STAR Collaboration, *RHIC Beam Use Request For Runs 17 and 18*, internal document, cit. 2.6.2016.

[7] D. Kharzeev, *Theoretical outlook*, QCD Workshop on Chirality, Vorticity, and Magnetic Field In Heavy Ion Collisions, UCLA, 2015

[8] The STAR Collaboration, *Memorandum of Understanding between the STAR and RHICf collaborations*, internal document, cit. 2.6.2016.

[9] K.H. Ackermann, N. Adams, C. Adler, et al., *STAR detector overview*, Nucl.Instrum.Meth., vol. A499, pp. 624–632, 2003

[10] C. Yang, X. J. Huang, C. M. Du, et al., *Calibration and performance of the STAR Muon Telescope Detector using cosmic rays*, Nucl.Instrum.Meth., vol. A762, pp. 1-6, 2014

[11] STAR Collaboration, *STAR Muon Telescope Detector Proposal, 2010*, http://www.star.bnl.gov/~ruanlj/MTDreview2010/MTD_proposal_v14.pdf.

[12] M. Beddo, E. Bielick, T. Fornek, et al., *The STAR Barrel Electromagnetic Calorimeter*, Nucl.Instrum.Meth., vol. A499, pp. 725-739, 2003

[13] Kohei Kajimoto, *A Large Area Time of Flight Detector for the STAR Experiment at RHIC. PhD thesis, The University of Texas in Austin, 2009*, http://repositories.lib.utexas.edu/handle/2152/7860.

[14] STAR Collaboration, *Pion, kaon, proton and anti-proton transverse momentum distributions from p+p and d+Au collisions at 200 GeV*, Phys. Lett. B 616, pp. 8-16, 2005

[15] M. Andersona, J. Berkovitzb, W. Betts, et al., *The STAR time projection chamber: a unique tool for studying high multiplicity events at RHIC*, Nucl.Instrum.Meth., vol. A499, pp. 659–678, 2003

[16] STAR Collaboration, *A Proposal for STAR Inner TPC Sector Upgrade (iTPC), 2015*, Cit. 22.6.2015 `https://drupal.star.bnl.gov/STAR/files/STAR_iTPC_proposal_06_09_2015.pdf`.

[17] K.A. Olive et al. (Particle Data Group), *Review of Particle Physics, Chin. Phys. C, 38, 090001 (2014)*, `http://pdg.lbl.gov/2014/reviews/rpp2014-rev-passage-particles-matter.pdf`.

[18] D.Beavis et.al., *The STAR Heavy Flavor Tracker Technical Design Report, 2011*, Cit. 19.3.2015, `https://drupal.star.bnl.gov/STAR/system/files/HFT_TDR_Final.pdf`.

[19] M. Szelezniak, *Upgrade of the STAR silicon detectors*, Vertex 2014, Doksy, Czech Republic

[20] Spiros Margetis, *Star Heavy Flavor Tracker*, QCD@WORK, Bari, Italy 2014

[21] M. Šimko, Λ_c *baryon production in Au+Au collisions at* $\sqrt{s_{NN}}$ = 200 GeV, Quark Matter, Kobe, Japan 2015

[22] G. Van Buren, *Developments in Tracking with STAR's Heavy Flavor Tracker*, Cit. 28.6.2015, Vertex 2015, Santa Fe, USA

[23] J. Bielčík, *Osobní konzultace*

[24] A. Besson, *DIGMAPS: a standalone tool to study digitization an overview of a digitizer strategy for CMOS/MAPS sensors*, cit. 28.3.2016 `http://phys.kent.edu/~smargeti/STAR/HFT/Work/Simulation_besson.pdf`

[25] M. Šimko, *Simulations for the HFT–Pixel detector at the STAR experiment*, Cit. 28.3.2016, Vertex 2014, Macha Lake, Czech Republic

[26] M. Lomnitz, *Measurement of D-meson azimuthal anisotropy in Au+Au 200GeV collisions at RHIC*, Quark Matter, Kobe, Japan 2015

[27] K.A. Olive et al. (Particle Data Group), *Review of Particle Physics, Chin. Phys. C, 38, 090001 (2014) and 2015 update*, `http://pdg.lbl.gov/2015/listings/rpp2015-list-D-plus-minus.pdf`.

[28] M. Lomnitz, *Private Communication*, 2016